Report No. 2

AN ANALYSIS OF THE GSFC LASER RANGING DATA

S.J. Moss
W.T. Wells

18 May 1967

prepared by

THE APPLIED SCIENCES DEPARTMENT
RESEARCH AND DEVELOPMENT CORPORATION
BLADENSBURG - MARYLAND

for

NATIONAL AERONAUTICS AND SPACE ADMINISTRATION

Contract No. 9756-58

AN ANALYSIS OF THE GSFC LASER RANGING DATA

S.J. Moss
W.T. Wells

May 18, 1967

Contract No. 9756-58

Prepared by: The Applied Sciences Department
Wolf Research and Development Corp.
Bladensburg, Maryland

Prepared for: The Optical Systems Branch
NASA Goddard Space Flight Center
Greenbelt, Maryland

Approved by W.T. Wells
Dept. Manager

TABLE OF CONTENTS

1.0 INTRODUCTION

This report describes the results of an extensive analysis of several sets of laser tracking data from the BE-C and GEOS-A satellites. The Laser Tracking System at Goddard Space Flight Center obtained the data. The report also discusses the analytical and statistical techniques used to analyze data from a single highly accurate tracking system whose primary measurement is the slant range from the tracker to the satellite.

The development of a new and highly accurate tracking system, such as the Goddard Laser System, presents some special problems in verifying its accuracy. Verification requires comparing the system to a more accurate reference system. This type of "yardstick" is not available; therefore, various indirect techniques must be used. First, one must find some estimate of the statistical character of the high frequency errors in the measurements. To obtain this estimate, one can fit an orbit to the observed data and investigate deviations in the measurements from the fitted orbit. If the measurement residuals do not exhibit significant serial correlation and if the average residual is small, e.g., $\leq$ .1 meter, one may conclude that the square root of the average square

residual is a good estimate of the standard deviation of the measurement. One may also conclude that the measurement if free from systematic errors except those that can be effectively masked by a short arc orbital fit. A study to determine the type of systematic errors that can be effectively masked by a short arc orbital fit shows that the orbital parameters are amazingly successful in adjusting out many combinations of the low frequency systematic results. Moreover, all types of systematic error(s) investigated can be removed except serially correlated errors. The results of the short arc orbital fits are discussed in Section 3.1.

To investigate the data and further for the presence of systematic errors, one must have nearly simultaneous data from another tracking system of high accuracy. Data was available on one of the passes considered from the Navy TRANET Doppler Tracking System in Howard County, Maryland. This data furnished an excellent comparison for further detecting possible systematic errors in the laser data. Results of orbital fits with the TRANET data as well as results of simultaneous fits with TRANET and laser data are described in Section 4.0.

2.0 THE DIFFERENTIAL CORRECTION PROCESS

To give those unfamiliar with tracking data analysis some understanding of the procedures followed to arrive at the results presented here, the rudiments of the Bayesian minimum variance procedure used in orbit determination are outlined below. We will restrict ourselves here to the estimation of only orbital parameters which we will denote, for generality, by x_i, $i = 1, \ldots 6$. These may be rectangular inertial coordinates, classical Keplerian elements, or any choice of six independent variables capable of describing the position and velocity of the satellite at a given instant. The goal of the estimation is to determine the set of orbital parameters at a given time t_o (called epoch) which produces the trajectory best fitting the measurements in the minimum variance sense. The analysis described herein can be easily extended to include the estimation of other parameters, such as station position of trackers and instrumentation error model parameters.

The orbit determination problem falls into the category of the non-linear estimation problem; i.e., the measurements from which the orbit is to

be deduced are not expressible as linear functions of the unknowns (x_i, i = 1, ... 6). This non-linearity requires that the estimation procedure be iterative rather than strictly analytic as in the linear case. A further complication arises because the equations of motion which apply to the near-earth satellite problem are not, in general, solvable in closed form but are required to be integrated numerically.

The two basic parts of any orbit determination program are the Orbit Generator and the Estimator. We will briefly discuss each of these in turn.

2.1 The Orbit Generator

The orbit generator, using a nominal or first guess set of elements at epoch, is used to numerically integrate the equations of motion to give the position and velocity of the satellite at any time t. Of particular interest is the predicted position and velocity at the times when measurements from tracking instrumentation are available. The differential correction process iteratively corrects the nominal elements by minimizing the sum

of squared differences between observed and computed measurements. The latter are calculated from the predicted x_i.

The orbit generator also provides some of the partial derivatives required by the estimator section. These derivatives are of the form:

$$\frac{\partial x_i(t)}{\partial x_j(t_o)} \quad i = 1,\ldots 6;\ j = 1,\ldots 6 \qquad (2.1)$$

where $x_i(t)$ are the position and velocity at time t (a measurement time) while $x_i(t_o)$ are those at epoch. For all but a few special cases (e.g., the two body central force problem and the inclusion of the J_2 term in the earth's potential) the partial derivatives given above are not available in closed form and therefore must be determined by numerical methods. These derivatives are created by integrating, in addition to the six differential equations (one for each x_i) of the nominal orbit, six additional sets of six differential equations with one of the $x_i(t_o)$ perturbed in turn. If the perturbation is denoted by $\Delta x_i(t_o)$

and the position and velocities of the perturbed orbits by $x_i'(t)$, the thirty-six partial derivatives are approximated by:

$$\frac{x_i'(t) - x_i(t)}{x_j(t_o)} \quad i = 1,\ldots 6;\ j = 1,\ldots 6 \qquad (2.2)$$

After each successive estimation, the set of corrected elements is returned to the orbit generator, and the above procedures are repeated.

2.2 The Estimator

The estimation procedure which is described here is of the Bayesian minimum variance type; i.e., the estimation criteria is based not only on the estimate of the noise of the measurements but also on an *a priori* uncertainty in the estimate of the unknowns. For example, in estimating

orbital elements, x_i, an uncertainty in the nominal values of these is used in the process. If the uncertainty in x_i is σ_{x_i}, a typical a priori weighting matrix is of the form:

$$\sum_o = \begin{bmatrix} \sigma^2_{x_1} & \sigma_{x_1x_2} & \sigma_{x_1x_3} & \cdots & \sigma_{x_1x_6} \\ \sigma_{x_2x_1} & \sigma^2_{x_2} & \sigma_{x_2x_3} & \cdots & \sigma_{x_2x_6} \\ \sigma_{x_3x_1} & \sigma_{x_3x_2} & \sigma^2_{x_3} & \cdots & \sigma_{x_3x_6} \\ \vdots & \vdots & \vdots & & \vdots \\ \sigma_{x_6x_1} & \sigma_{x_6x_2} & \sigma_{x_6x_3} & & \sigma^2_{x_6} \end{bmatrix} \qquad (2.3)$$

The off-diagonal terms, which are the covariances of the x_i, are usually taken to be zero, because better information is not generally available.

The variance-covariance matrix is defined as:

$$V = [B^T \Sigma^{-1} B]^{-1} \tag{2.4}$$

In Beyesian form, i.e., taking account of prior information, this becomes,

$$V_B = [B^T \Sigma^{-1} B + \Sigma_o^{-1}]^{-1} \tag{2.5}$$

The matrix B is an array of partial derivatives of the measurements with respect to the unknowns, thus, if there are j measurements and i unknowns, B is dimensioned j x i. For our problem of estimating only orbital parameters, B would appear as

$$B = \begin{bmatrix} \frac{\partial m_1}{\partial x_1(t_o)} & \frac{\partial m_1}{\partial x_2(t_o)} & \frac{\partial m_1}{\partial x_3(t_o)} & \cdots \\ \frac{\partial m_2}{\partial x_1(t_o)} & \frac{\partial m_2}{\partial x_2(t_o)} & \cdots & \\ \vdots & & & \\ \frac{\partial m_j}{\partial x_1(t_o)} & \frac{\partial m_j}{\partial x_2(t_o)} & & \frac{\partial m_j}{\partial x_6(t_o)} \end{bmatrix} \quad (2.6)$$

Two points should be mentioned here:

1. Note that the measurement m_j is made at some time $t \neq t_o$ so that the partial derivatives must be constructed as follows:

$$\frac{\partial m_j(t)}{\partial x_i(t_o)} = \sum_{k=1}^{6} \frac{\partial m_j(t)}{\partial x_k(t)} \quad \frac{\partial x_k(t)}{\partial x_i(t_o)} \qquad (2.7)$$

Whereas the derivatives $\frac{\partial m_j(t)}{\partial x_k(t)}$

are available in closed form, the

derivatives $\frac{\partial x_k(t)}{\partial x_i(t_o)}$ are obtained

numerically from the orbit generator. See Section 2.1.

2. There may be more than one measurement at a given time t. These may be from a single station, e.g., measuring range, azimuth and elevation, or from a number of stations making single or multiple measurements while viewing the satellite simultaneously.

The matrix $\sum$ is a matrix which reflects the relative weight of each measurement. In general, the measurement noise, σ_j, is used so that

$$\sum = \begin{bmatrix} \sigma_1^2 & o & o & o & o & o \\ o & \sigma_2^2 & . & . & . & . \\ . & & & & & \\ . & & & & & \\ . & & & & & \\ . & & & & & \\ & & & & & \sigma_j^2 \end{bmatrix} \qquad (2.8)$$

and is a j x j matrix.

The correction to the most recent nominal values of the unknowns can now be made. Letting $m_{j\ obs}$ and $m_{j\ cal}$ be the measured value of the observation m_j and $m_{j\ cal}$, the calculated value based on the nominal values of $x_i(t_o)$, we construct the residual column vector ε:

$$\varepsilon = \begin{bmatrix} m_{1\ obs} - m_{1\ cal} \\ m_{2\ obs} - m_{2\ cal} \\ \vdots \\ m_{j\ obs} - m_{j\ cal} \end{bmatrix} \tag{2.9}$$

The correction, δ, to the most recent best estimate of the nominal elements is then given by:

$$\delta = [B^T \Sigma^{-1} B + \Sigma_o^{-1}]^{-1} B^T \Sigma^{-1} \varepsilon. \qquad (2.10)$$

Thus, δ is simply a column vector with six elements

$$\delta = \begin{bmatrix} \Delta x_1 \\ \Delta x_2 \\ \Delta x_3 \\ \Delta x_4 \\ \Delta x_5 \\ \Delta x_6 \end{bmatrix} \qquad (2.11)$$

each of which is added algebraically to the corresponding last nominal element.

Each successive iteration is begun with the new element set but with the original a priori matrix. Termination of the iteration process can be on one of a number of criteria some of which are:

1. Value of the mean of residuals,
2. Percentage change in the unknowns from iteration to iteration,
3. Value of the weighted sum of squares of observational residuals.

The elements of V_B provide information on the standard deviation in the estimates of the unknowns and the corresponding correlations between them. Noticing that V_B is symmetric and denoting its elements by v_{nm}, the standard deviation in the i^{th} unknown is given by:

$$\sigma_i = \sqrt{v_{ii}} \tag{2.12}$$

while the correlation between the estimates of the i^{th} and j^{th} unknowns is

$$\rho ij = \frac{v_{ij}}{\sigma_i \sigma_j} \tag{2.13}$$

2.3 The GDOP

The interpretation of the matrix V_B by itself is also interesting because it forms the basis of the error analyses often called GDOP's (Geometrical Dilution of Precision). Frequently, it is important to know how well a given station configuration tracking a satellite in a specified orbit can recover parameters of interest. By choosing a set of elements and associated uncertainties in these at epoch, a station geometry, measurements types, noise level and frequency of the measurements, the covariance matrix evaluated for this simulation provides information on parameter recovery capability. This procedure provides values for the standard deviations in the estimates and correlation between estimates of the unknowns without actually estimating their value. One understands the reason for this from the differential correction estimator in Section 2.2. Whereas the corrections are computed from the combination of the residual vector, ε, and the variance-covariance matrix, V_B, the standard deviation in the estimates of the unknowns and the correlations are found entirely from V_B.

The utility of the GDOP in mission analyses and planning is substantial. This procedure is easily expandable to include capability such as recovering station position and error model parameter.

3.0 SINGLE-STATION RANGE ONLY RESULTS

This section discusses the results obtained from fitting laser range measurements to a short arc of an orbit. The results presented were obtained from single-station observations of the satellites BE-C and GEOS-A. The BE-C data was taken from the Goddard Space Flight Center while the GEOS-A tracking was done from Rosman, North Carolina. In addition to the short arc results, a discussion of systematic error effects on these solutions is presented.

3.1 Short Arc Orbital Fit

The laser tracking data discussed in this section is comprised of range only measurements from a single observing station. These data were reduced using the WRDC Simultaneous Least Squares Adjustment of Parameters (SLAP), adjusting the orbit to the measurements in the minimum variance sense.

It is well known that, range only measurements are generally ambiguous when used in orbit estimation. This apparent impasse is overcome in

the SLAP program through the use of a priori information which acts to determine the direction from the observer to the satellite for the initial range measurements. Although the GSFC laser tracking system also measures azimuth and elevation angles, these measurements were not included in the reductions discussed in this section.

The purpose of the single station solutions was three-fold:

1. To determine the noise level of the laser range measurements

2. To determine whether the high sampling rate available from this instrument provides uncorrelated measurements

3. To establish the type of systematic errors that cannot be recovered from single station range only data and to determine those which might be recoverable.

The procedures used are presented below as they were executed.

Following the pre-processing of the raw data, Appendix A, Pre-Processing, the data was reduced in SLAP, adjusting the orbit until the range residuals were reduced to the order of ten or fifteen meters root mean square about the mean. At this point the residuals were manually edited by removing those points which were several sigma out. Generally, this amounted to less than five per cent of the points.

The edited data was then resubmitted to the SLAP program using the same a priori information and associated variances as in the initial reduction. The reduction of the remaining data, which provides the set of orbital elements giving the best fit to the measurements in the minimum variances sense, was continued until a convergence criterion was met. This criterion was that the average of the range residuals was less than 0.1 meter.

Before determining the true noise level in the data, one should establish whether the residuals are essentially random. If for example, the residuals test out to be serially correlated, an accurate estimate of the true noise is at best difficult to make. The appearance of systematic trends in the residuals can result from biases in

the measuring device and/or serial correlation in the measurement errors. Residuals appearing random allow for an estimate of the noise to be made. One should remember, however, that whether bias errors and/or serial correlation are masked by a single-station solution remains to be determined (Section 2.2). While the appearance of being random allows a good estimate of the noise, it may not guarantee that the measurements are unbiased and uncorrelated.

A simple "runs" test was applied to determine significant non-randomness. This test proceeds as follows.

Given N residuals, the number of times the residuals change sign is counted. For cases where N > 25 and the residuals are random, the number of sign changes n can be assumed normally distributed with mean or expected value,

$$\bar{n} = \frac{N + 1}{2} \qquad (3.1)$$

and the standard deviation,

$$\sigma = \sqrt{\frac{N(N-2)}{4(N-1)}} \quad . \tag{3.2}$$

Letting n_o be the observed number of sign changes, a normal deviate can be computed as follows:

$$z = \frac{n_o - \bar{n}}{\sigma} \quad . \tag{3.3}$$

This value of z is then compared to the tabulated values of the standard normal distribution to test for significant non-randomness of the residuals. For example,

$$\text{if} \quad |z| < 2.54 \ , \tag{3.4}$$

then the residuals can be considered not to be significantly non-random at the 99% confidence level.

The results of this investigation are presented below. Table 1 summarizes the data from each pass analyzed and gives the set of orbital elements found which best fit these data. In addition, the values of the normal deviate described previously are given. Figures 1 - 8 are plots of some of the range residuals. Normalized histograms of the residuals are also shown for a few of the passes. (Figures 9 - 14.) Figures 15 - 30 show the ground tracks and elevation profiles of the passes considered.

From these single-station range only orbital fits, several conclusions can be drawn:

1. The data examined to date have exhibited no statistically significant non-randomness, even at the sampling rate of one per second. This is significant in that it implies that the laser system is capable of providing a high density of uncorrelated measurements. It should be re-emphasized at this point, however, that it remains to be shown that the system is free of bias errors in spite of the random appearance of the residuals.

TABLE 1

Date	Satellite	Epoch	Range Noise (meters)	Random Normal Deviate	Semi Major Axis (meters)	Eccentricity	Inclination	Argument of Perigee	Right Ascension of Node	Mean Anomaly
4 May 66	BE-C	$01^h36^m57^s$	1.79	-0.05	7494829.4	0.025	40°.270	174°.560	106°.219	242°.533
4 May 66	BE-C	$03^h32^m42^s$	1.86	-0.70	7492165.3	0.025	41°.360	174°.040	108°.897	267°.620
5 May 66	BE-C	$00^h57^m53^s$	1.72	-1.96	7499208.0	0.025	40°.702	178°.285	103°.917	239°.937
5 May 66	BE-C	$02^h51^m07^s$	2.26	-1.95	7469718.8	0.025	41°.688	182°.395	105°.897	251°.640
9 Sep 66	GEOS-A	$01^h21^m26^s$	1.62	-2.00	8070887.1	0.072	59°.364	351°.618	131°.222	123°.619
10 Sep 66	GEOS-A	$01^h28^m29^s$	1.50	0.11	8073285.9	0.072	59°.356	352°.520	128°.970	135°.293
6 Oct 66	GEOS-A	$10^h31^m17^s$	2.22	0.22	8077083.6	0.072	59°.353	10°.065	69°.678	18°.025
7 Oct 66	GEOS-A	$10^h35^m25^s$	2.05	0.99	8075263.3	0.072	59°.436	10°.510	67°.510	18°.915
8 Oct 66	GEOS-A	$10^h38^m40^s$	1.60	1.61	8076610.8	0.072	59°.403	11°.161	65°.232	16°.960
15 Nov 66	GEOS-A	$11^h31^m12^s$	1.79	2.02	8091145.0	0.072	59°.102	36°.630	340°.119	90°.447
18 Nov 66	GEOS-A	$09^h37^m55^s$	1.22	0.00	8067134.5	0.072	59°.783	37°.0219	332°.600	78°.451
19 Nov 66	GEOS-A	$01^h12^m08^s$	2.53	-0.27	8076656.2	0.072	59°.389	38°.077	331°.732	352°.716
19 Nov 66	GEOS-A	$09^h41^m30^s$	1.65	-1.86	8068840.8	0.072	59°.466	37°.716	330°.807	77°.231
20 Nov 66	GEOS-A	$01^h16^m01^s$	1.78	0.76	8083782.5	0.073	59°.168	38°.693	329°.445	352°.745
20 Nov 66	GEOS-A	$09^h48^m28^s$	2.17	Too few points	8072472.7	0.072	59°.382	38°.654	328°.644	86°.114
21 Nov 66	GEOS-A	$01^h20^m22^s$	1.84	1.84	8101992.1	0.075	59°.024	34°.535	327°.054	354°.032

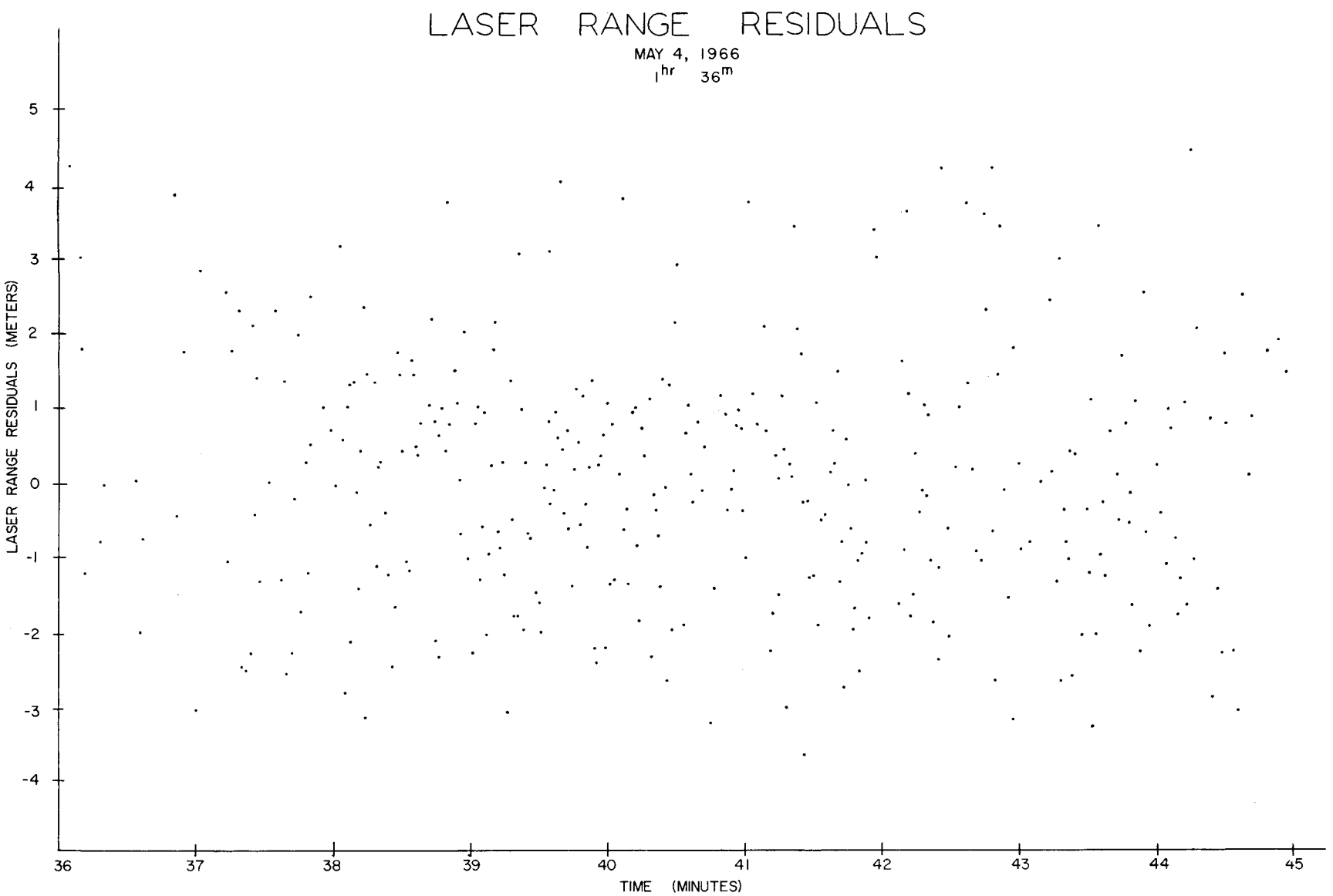
LASER RANGE RESIDUALS
MAY 4, 1966
1hr 36m
LASER RANGE RESIDUALS (METERS)
5
4
3
2
1
0
-1
-2
-3
-4
36
37
38
39
40
41
42
43
44
45
TIME (MINUTES)

Figure 1

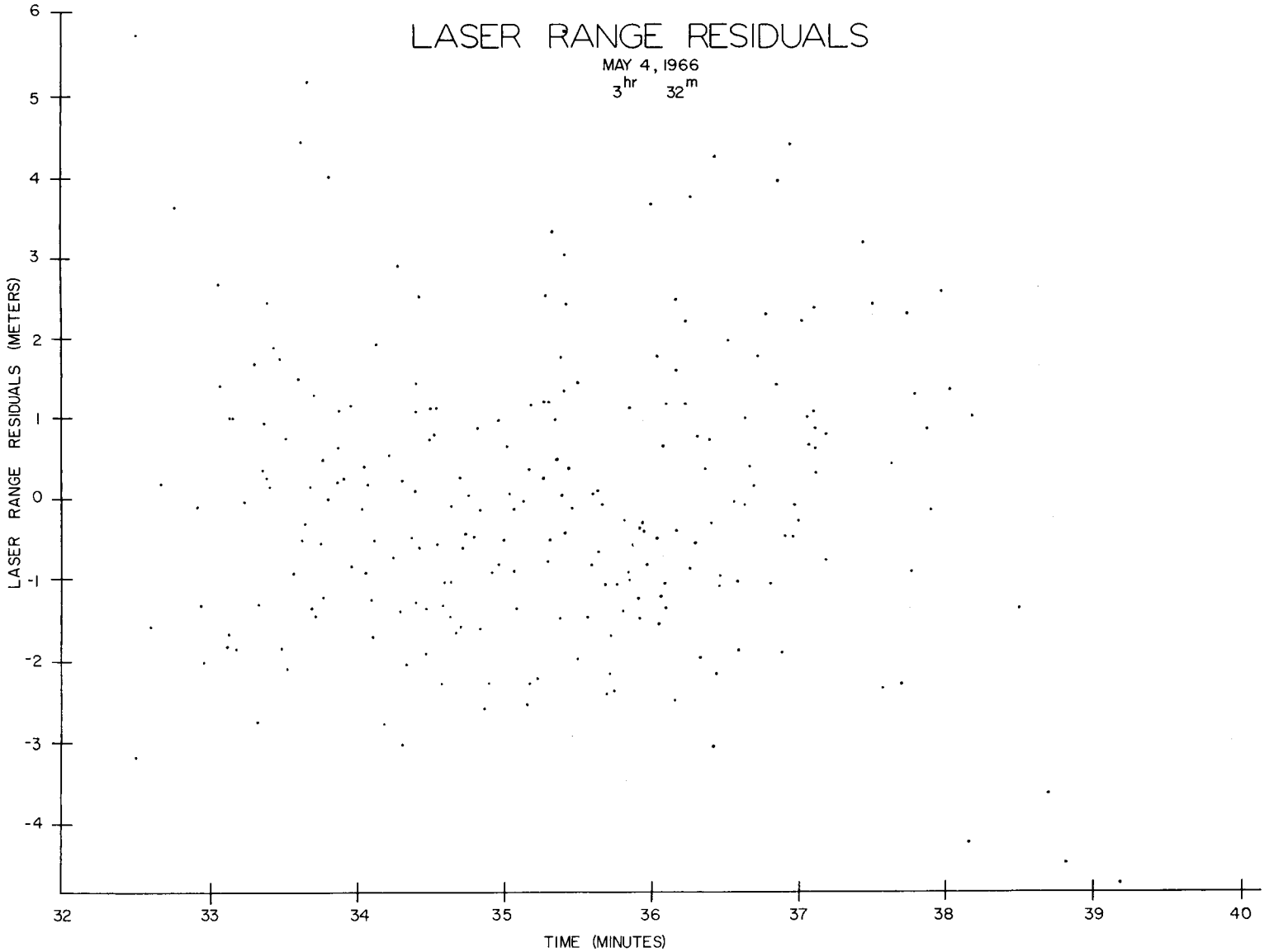
LASER RANGE RESIDUALS
MAY 4, 1966
3hr 32m
LASER RANGE RESIDUALS (METERS)
6
5
4
3
2
1
0
-1
-2
-3
-4
32
33
34
35
36
37
38
39
40
TIME (MINUTES)

Figure 2

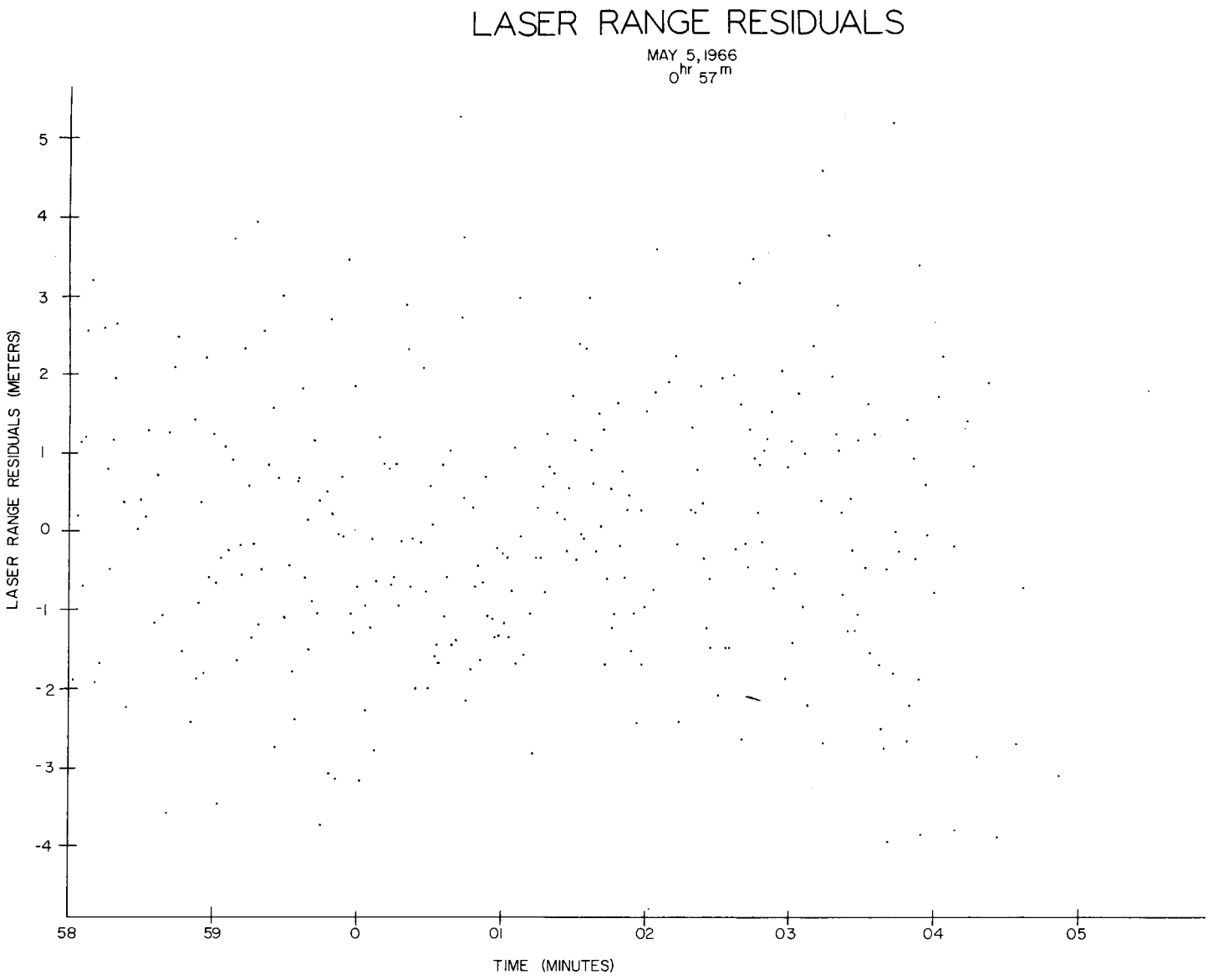
LASER RANGE RESIDUALS
MAY 5, 1966
0hr 57m
LASER RANGE RESIDUALS (METERS)
5
4
3
2
1
0
-1
-2
-3
-4
58
59
0
01
02
03
04
05
TIME (MINUTES)

Figure 3

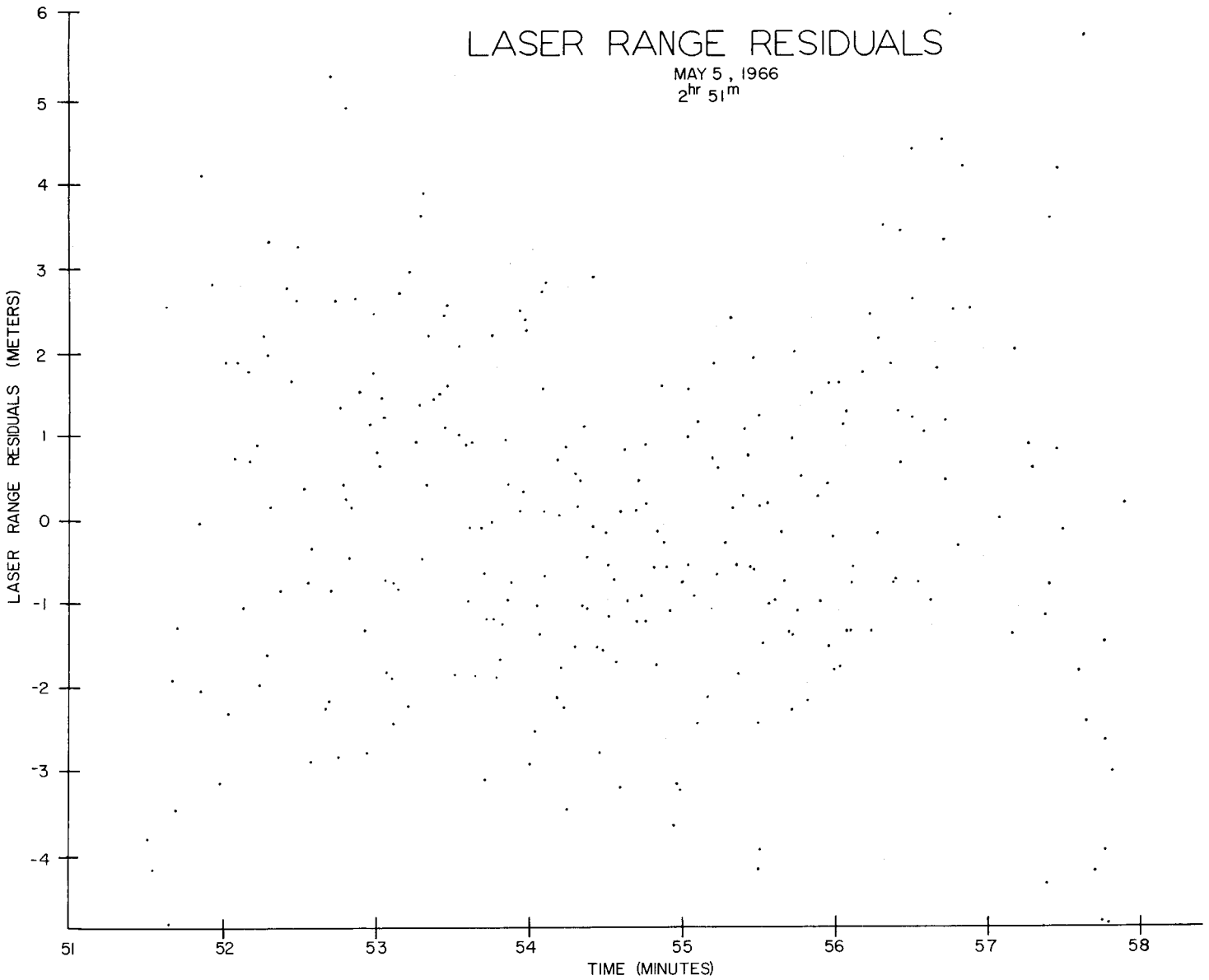
LASER RANGE RESIDUALS
MAY 5, 1966
2hr 51m
LASER RANGE RESIDUALS (METERS)
6
5
4
3
2
1
0
-1
-2
-3
-4
51
52
53
54
55
56
57
58
TIME (MINUTES)

Figure 4

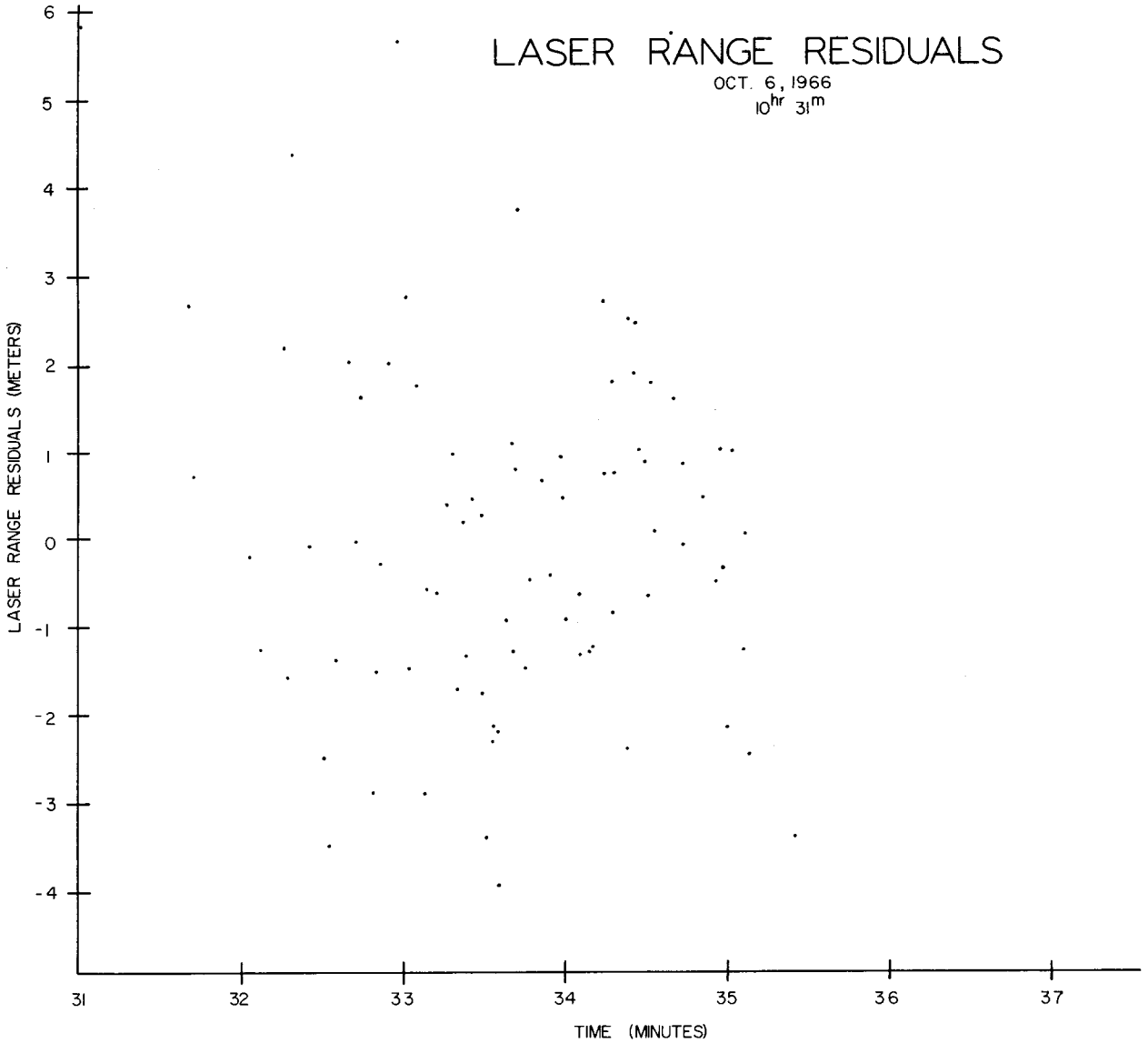
LASER RANGE RESIDUALS
OCT. 6, 1966
10hr 31m
LASER RANGE RESIDUALS (METERS)
6
5
4
3
2
1
0
-1
-2
-3
-4
31
32
33
34
35
36
37
TIME (MINUTES)

Figure 5

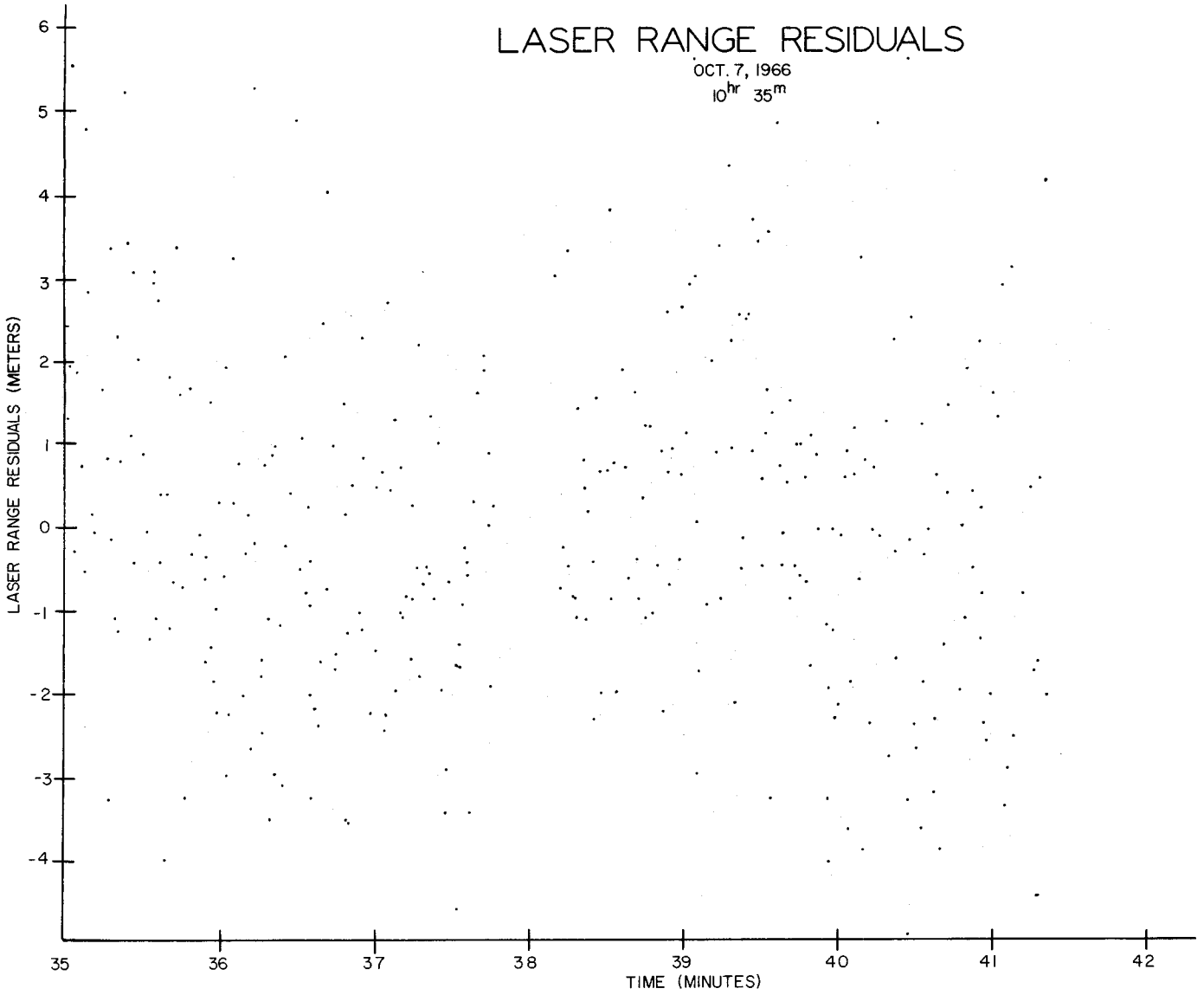
LASER RANGE RESIDUALS
OCT. 7, 1966
10hr 35m
LASER RANGE RESIDUALS (METERS)
6
5
4
3
2
1
0
-1
-2
-3
-4
35
36
37
38
39
40
41
42
TIME (MINUTES)

Figure 6

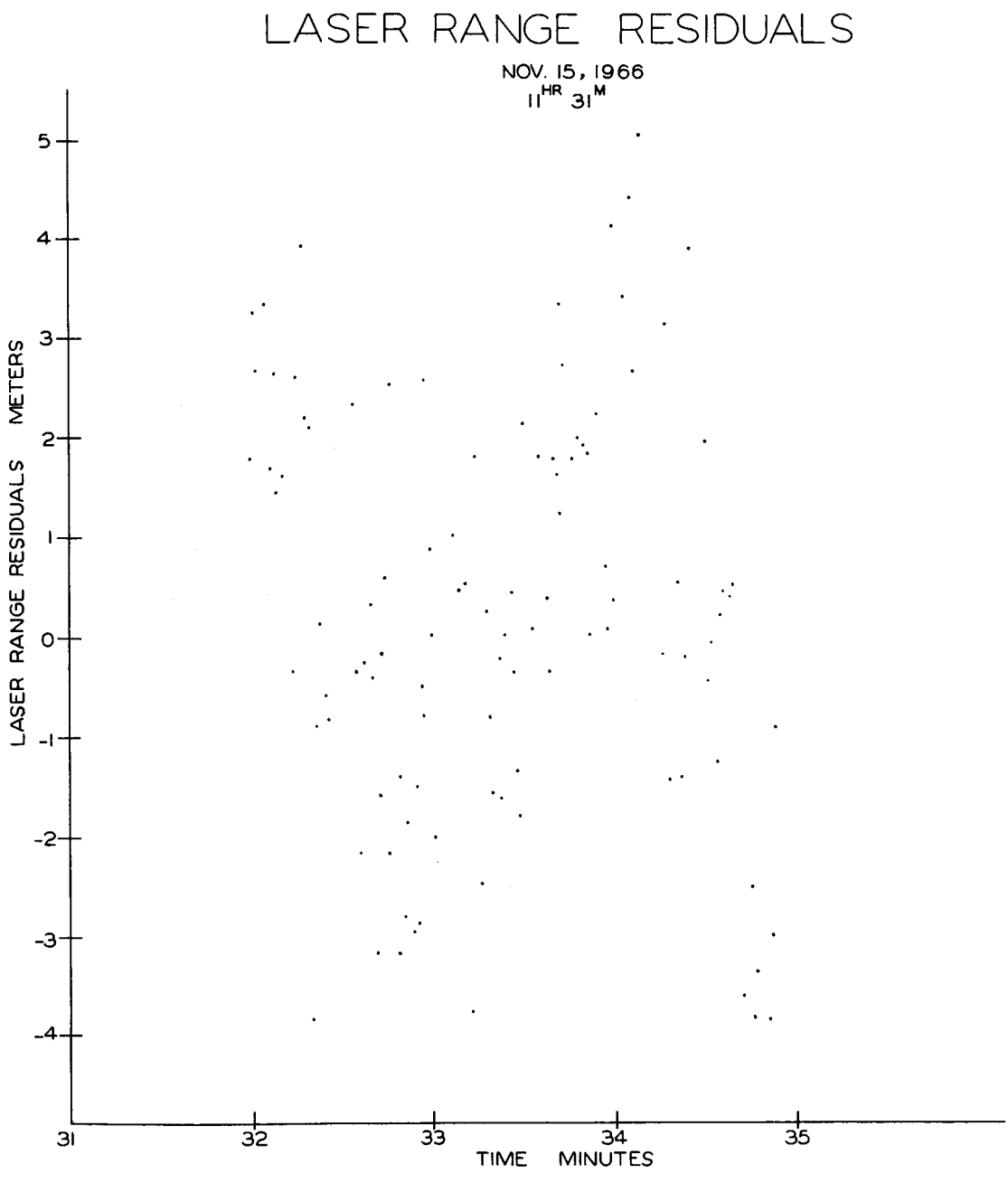
LASER RANGE RESIDUALS
NOV. 15, 1966
11HR 31M
LASER RANGE RESIDUALS METERS
5
4
3
2
1
0
-1
-2
-3
-4
31
32
33
34
35
TIME MINUTES

Figure 7

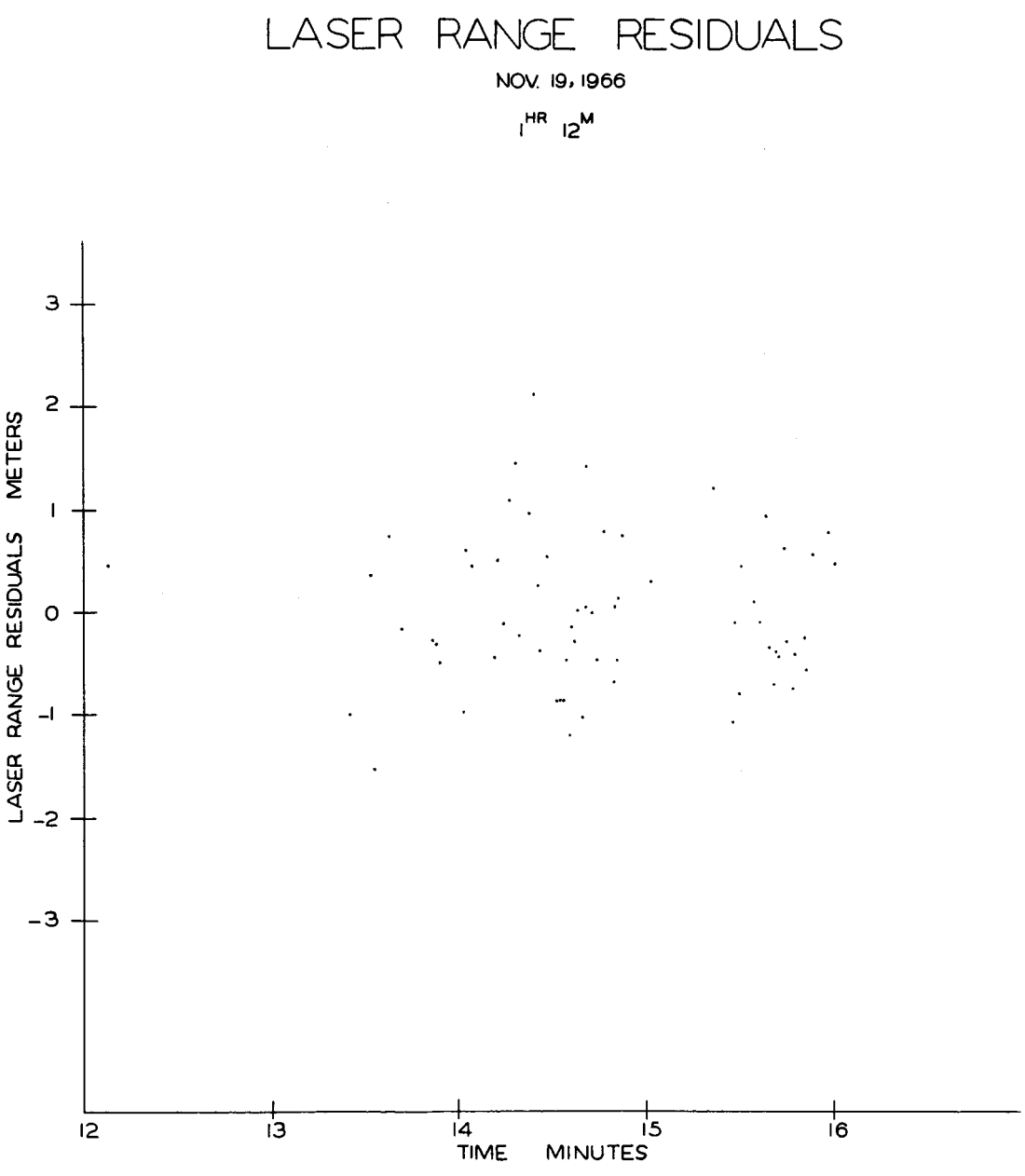
LASER RANGE RESIDUALS
NOV. 19, 1966
1HR 12M
LASER RANGE RESIDUALS METERS
3
2
1
0
-1
-2
-3
12
13
14
15
16
TIME MINUTES

Figure 8

May 4, 1966
$01^h\ 36^m\ 57^s$

Figure 9

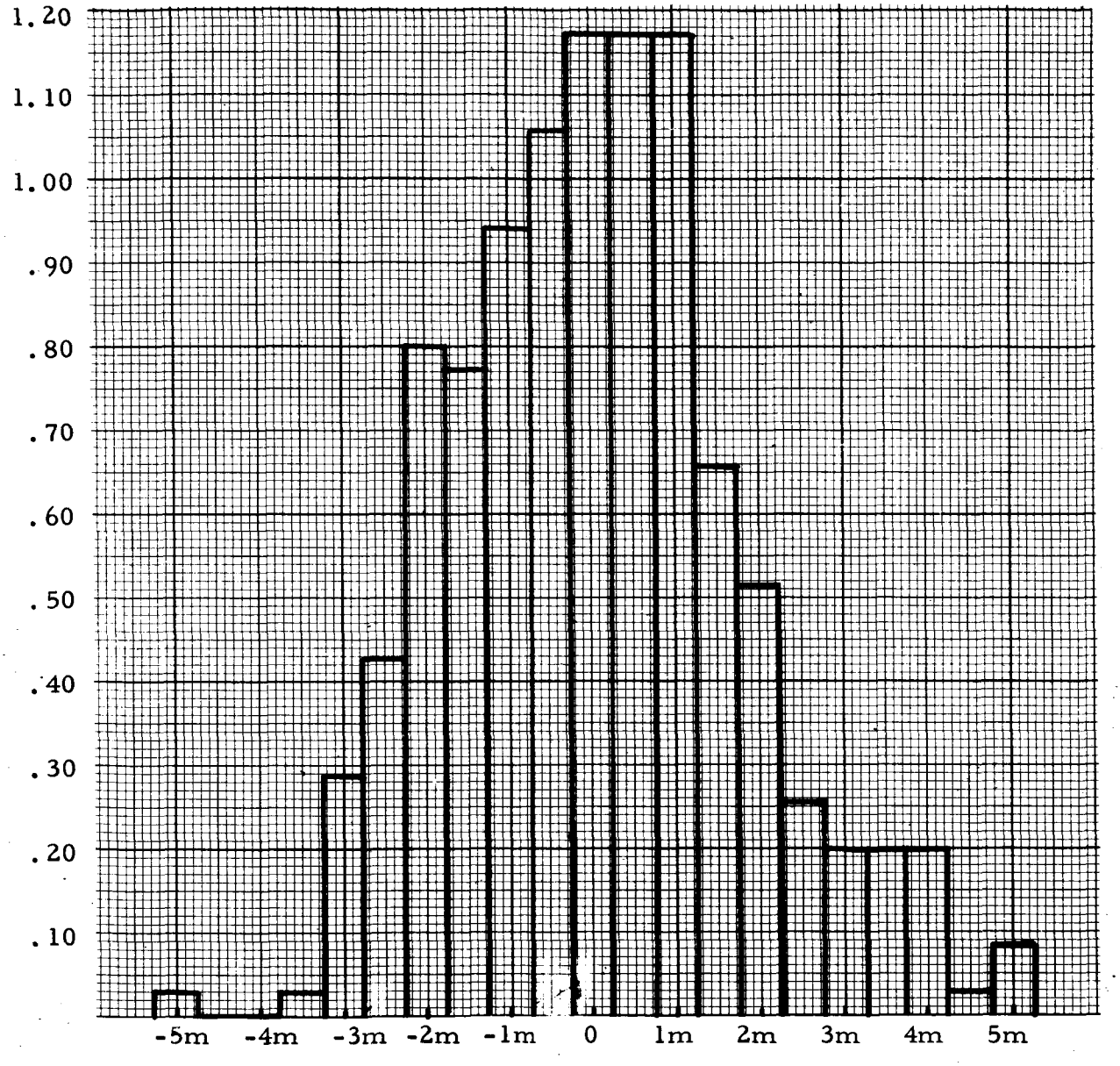

May 4, 1966
$03^h\ 32^m\ 42^s$

Figure 10

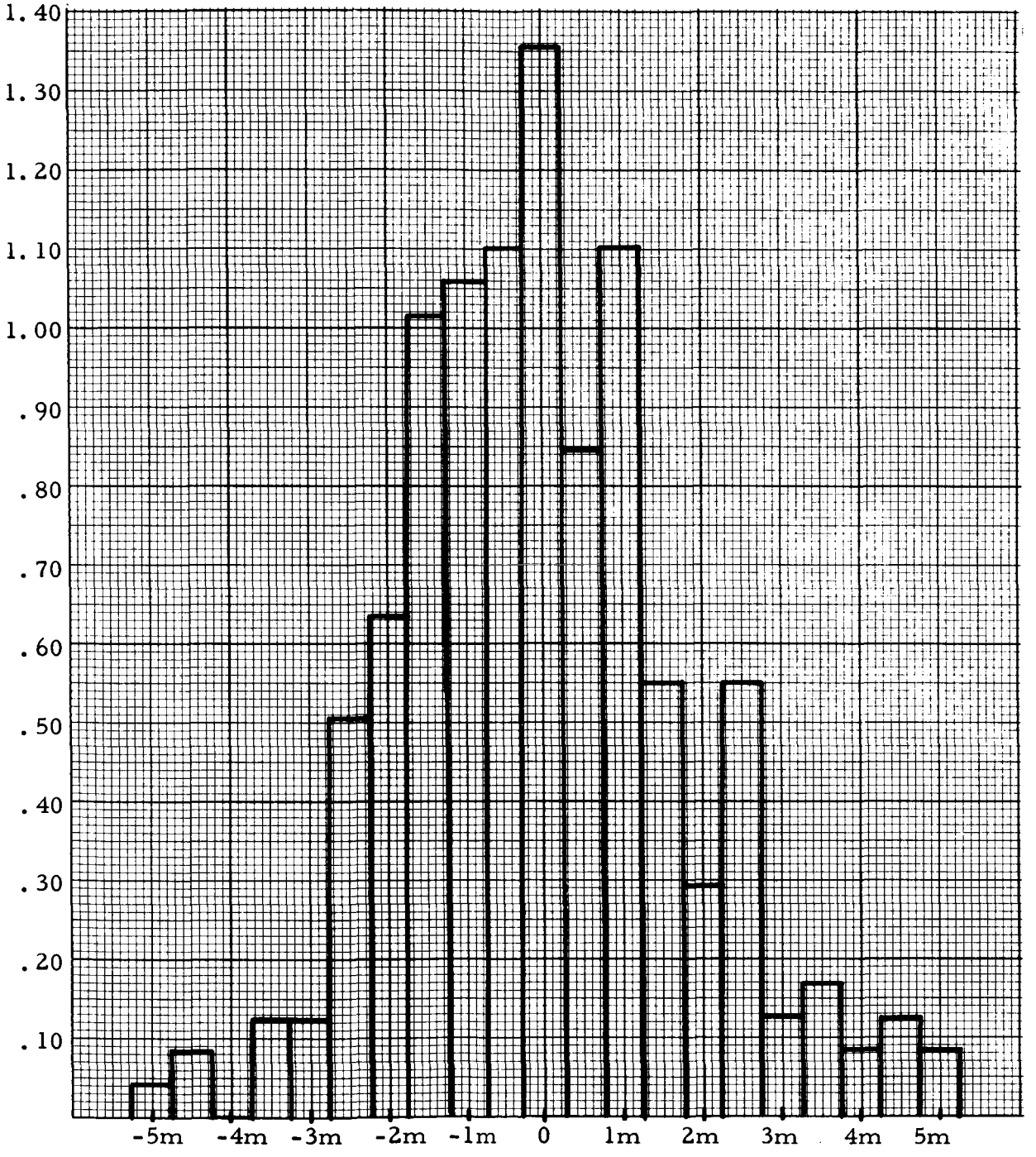

May 5, 1966
$0^h\ 57^m\ 53^s$

Figure 11

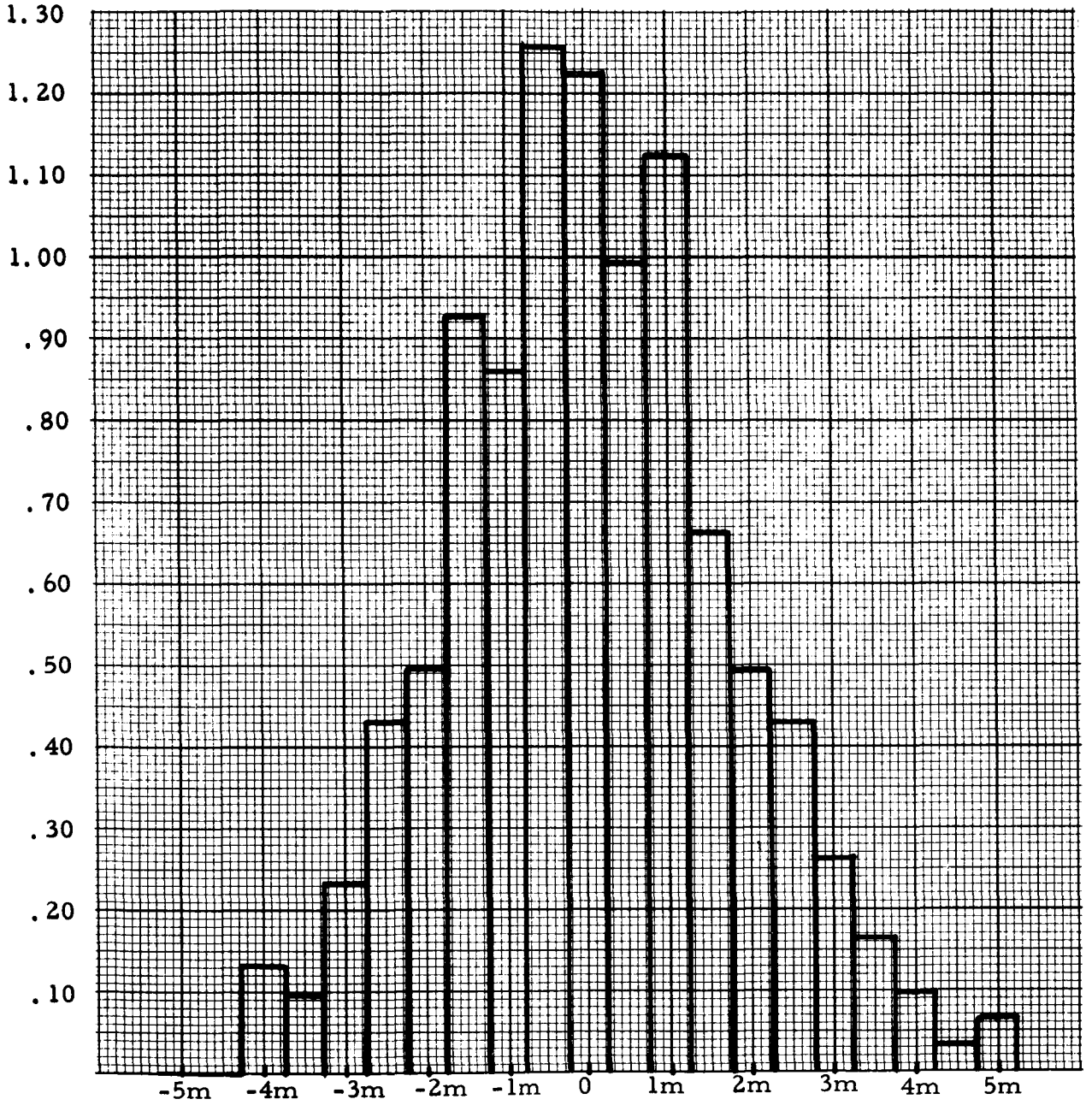

May 5, 1966
$02^h\ 51^m\ 7^s$

Figure 12

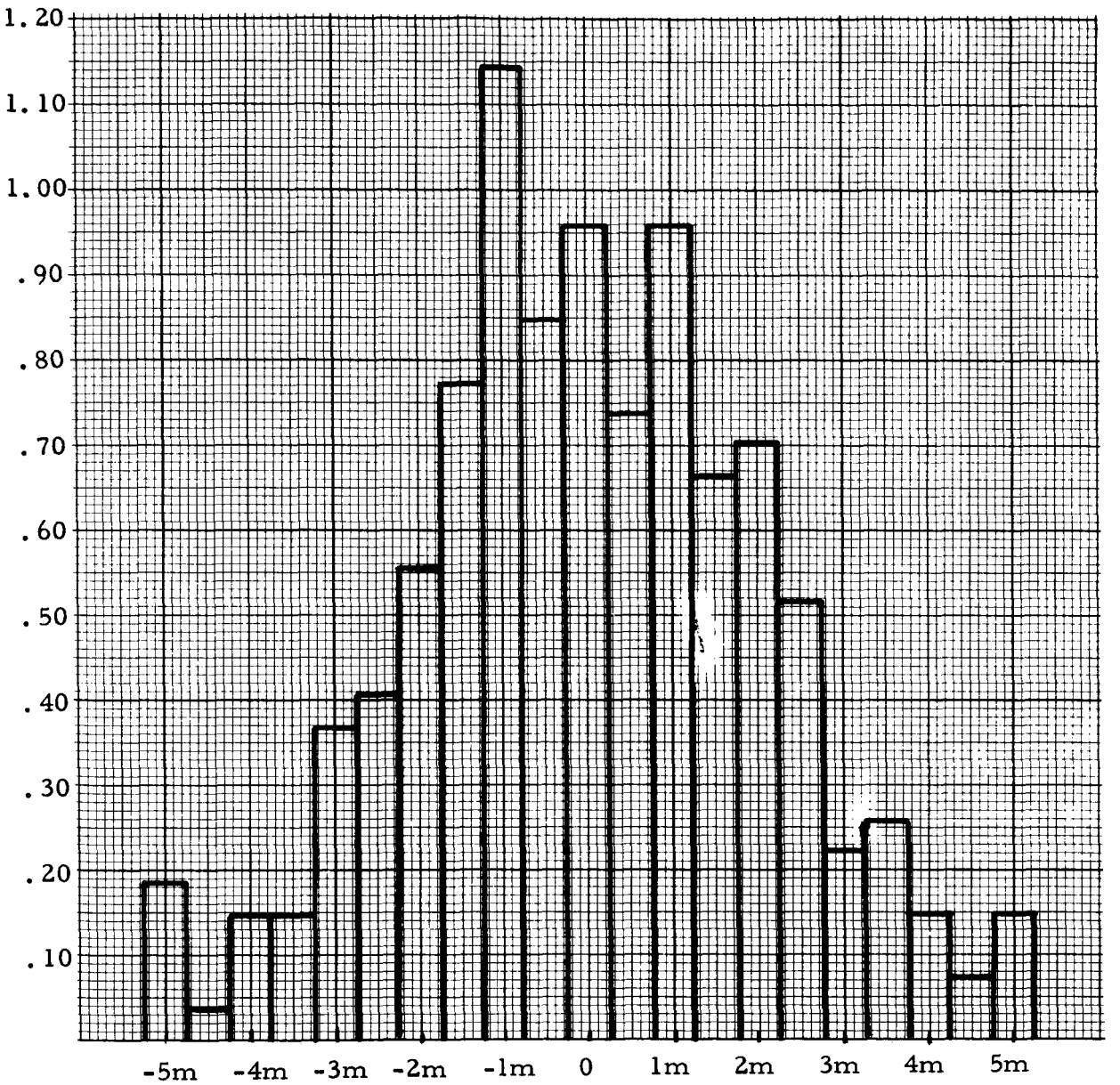

September 9, 1966
$01^h\ 19^m\ 57^s$
Figure 13

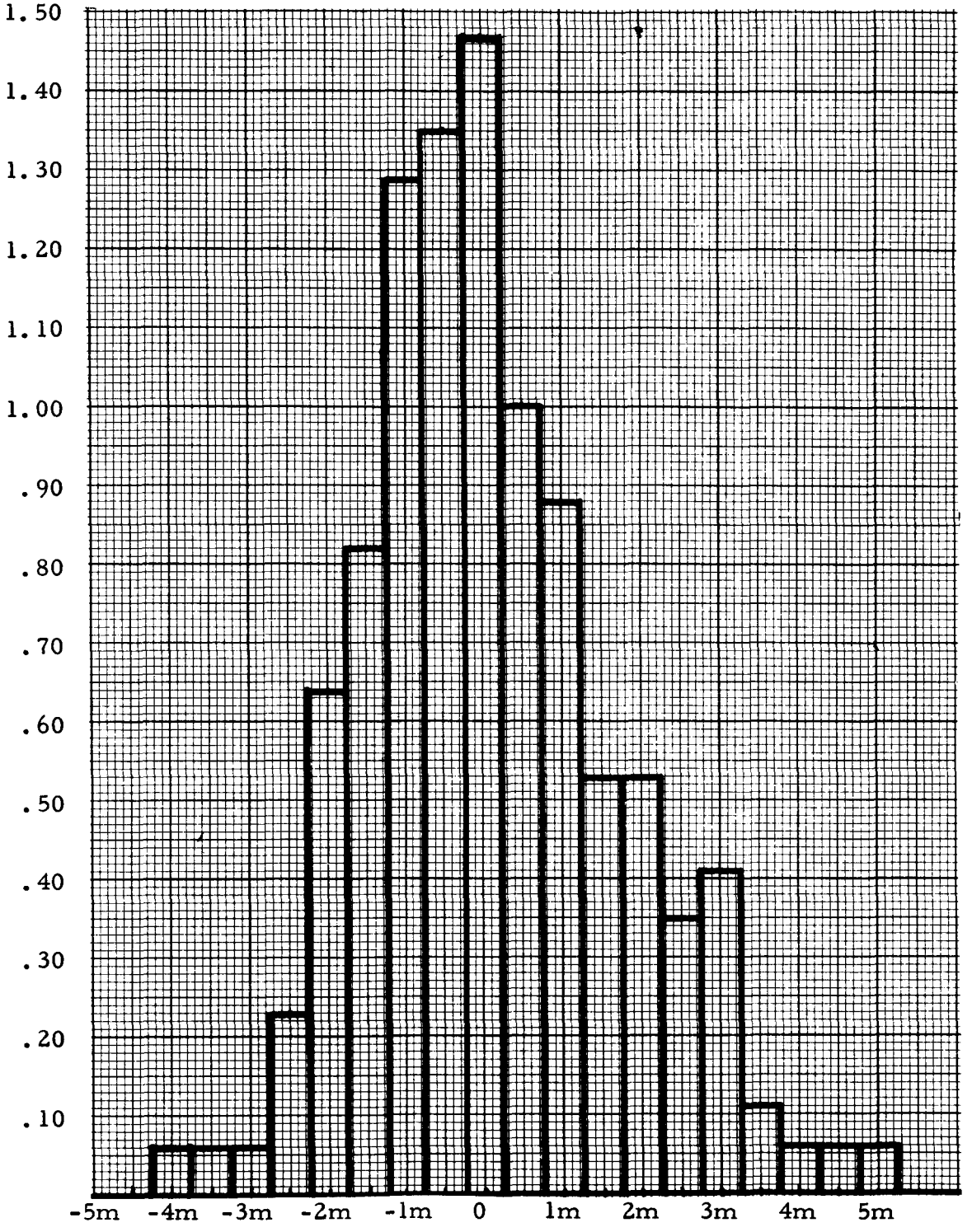

September 10, 1966
$01^h\ 27^m\ 50^s$

Figure 14

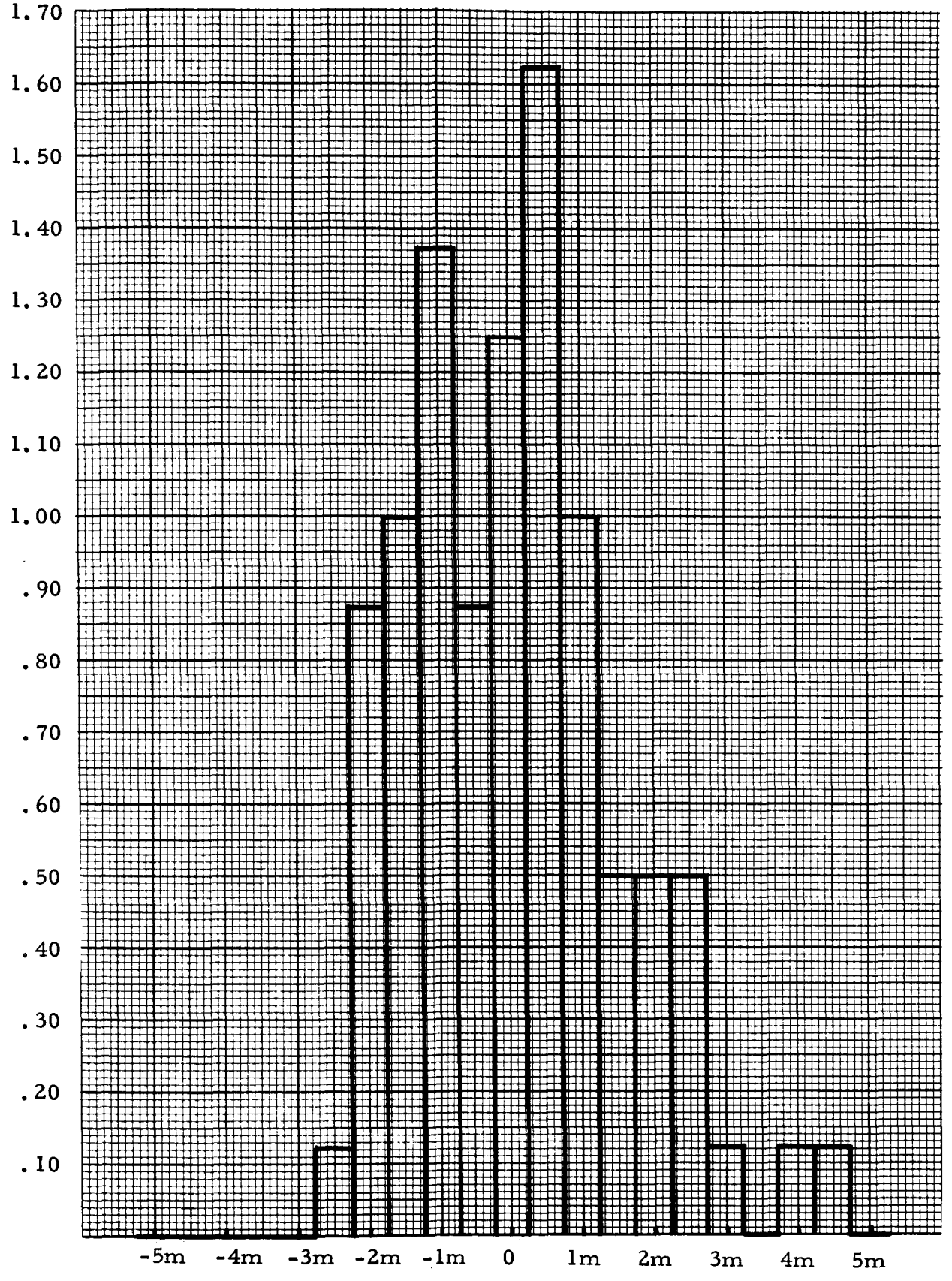

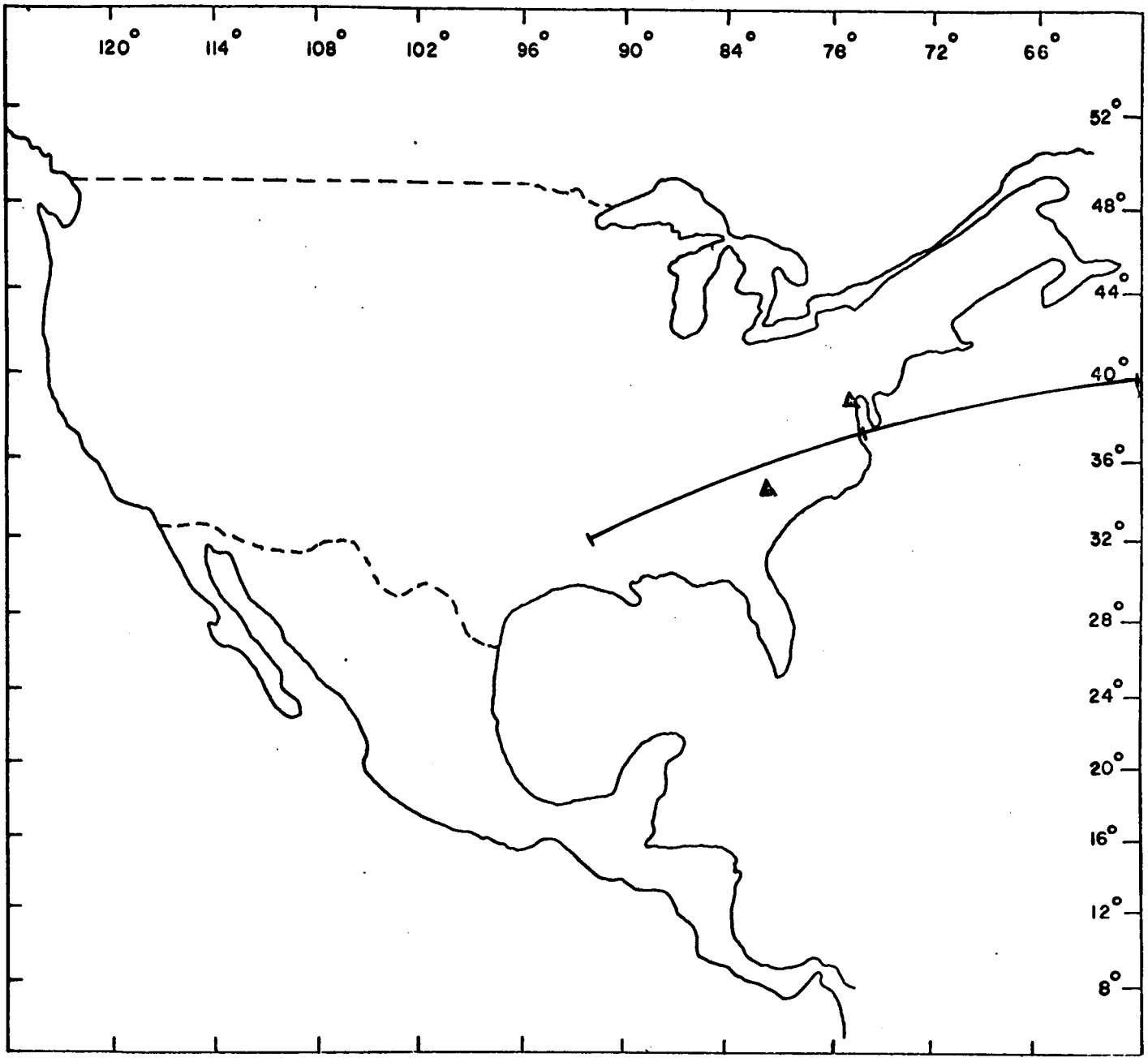

MAY 4 , 1966

BASE TIME
1.000 HOUR
36.000 MINUTES
57.00170 SECONDS

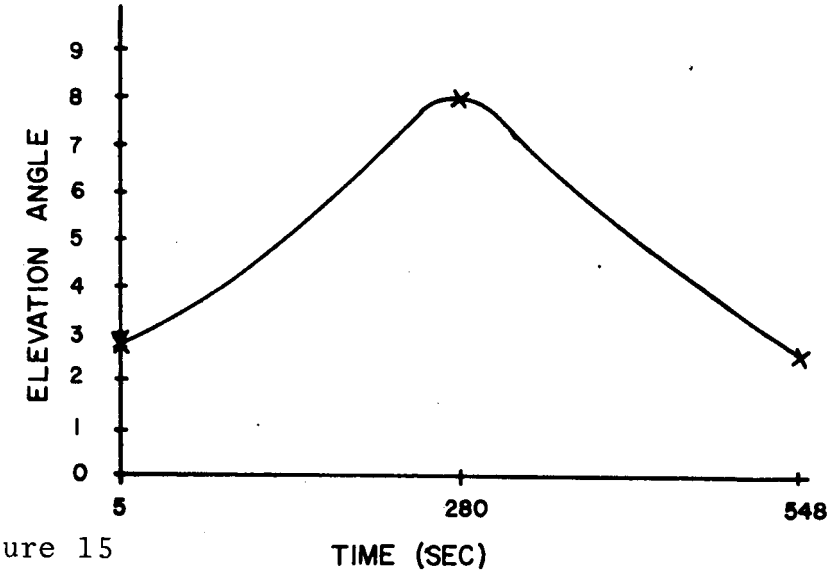

Figure 15

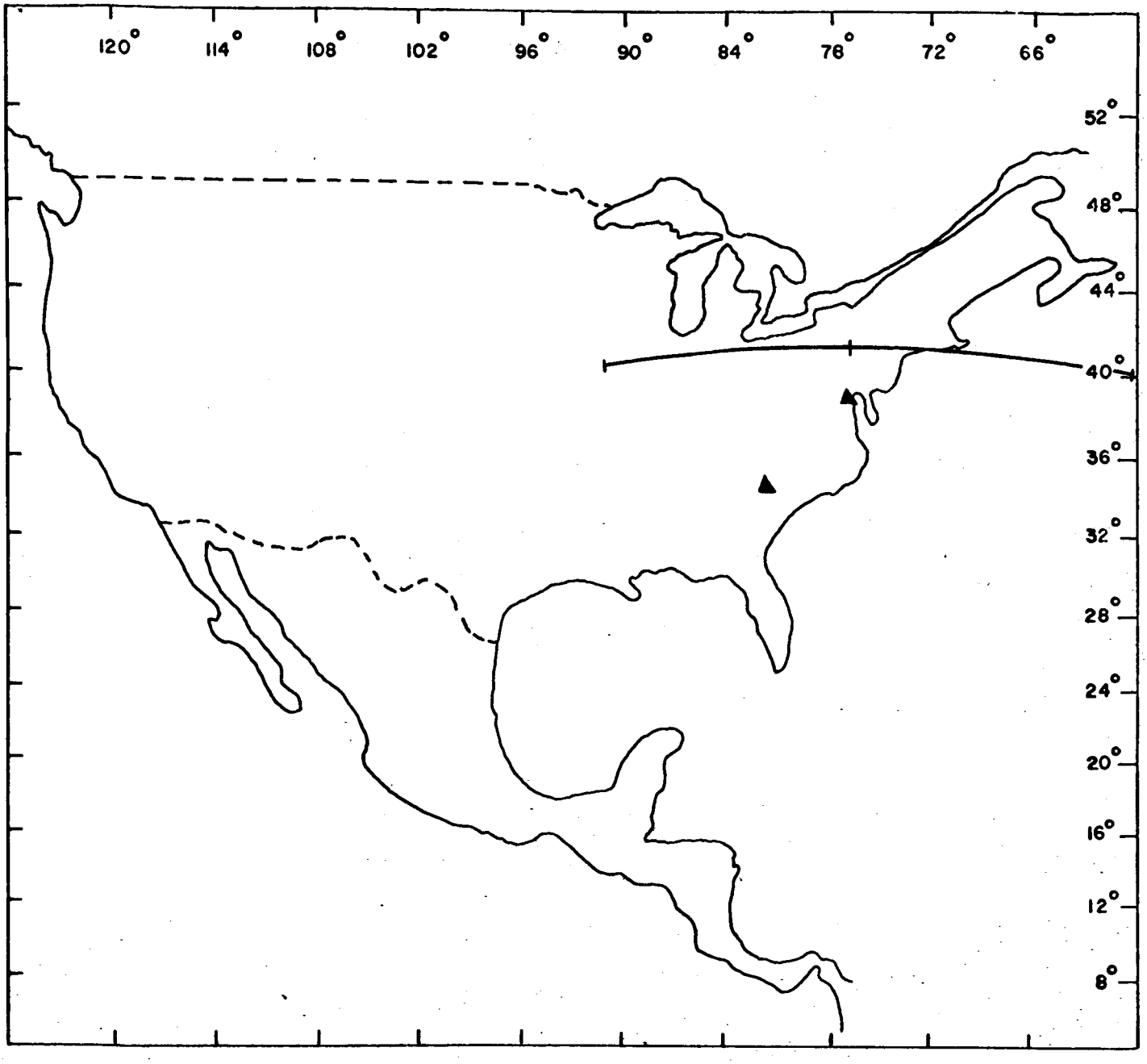

MAY 4, 1966

BASE TIME
3.000 HOURS
32.000 MINUTES
42.00730 SECONDS

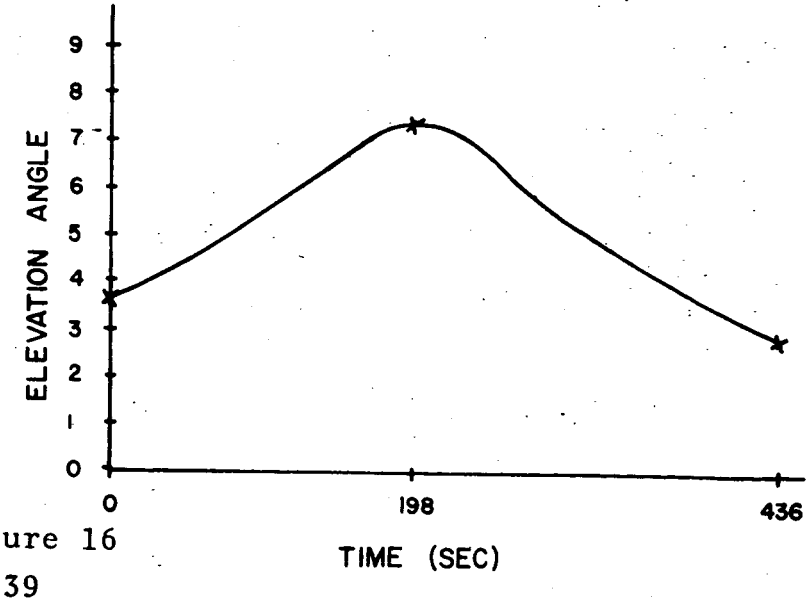

Figure 16

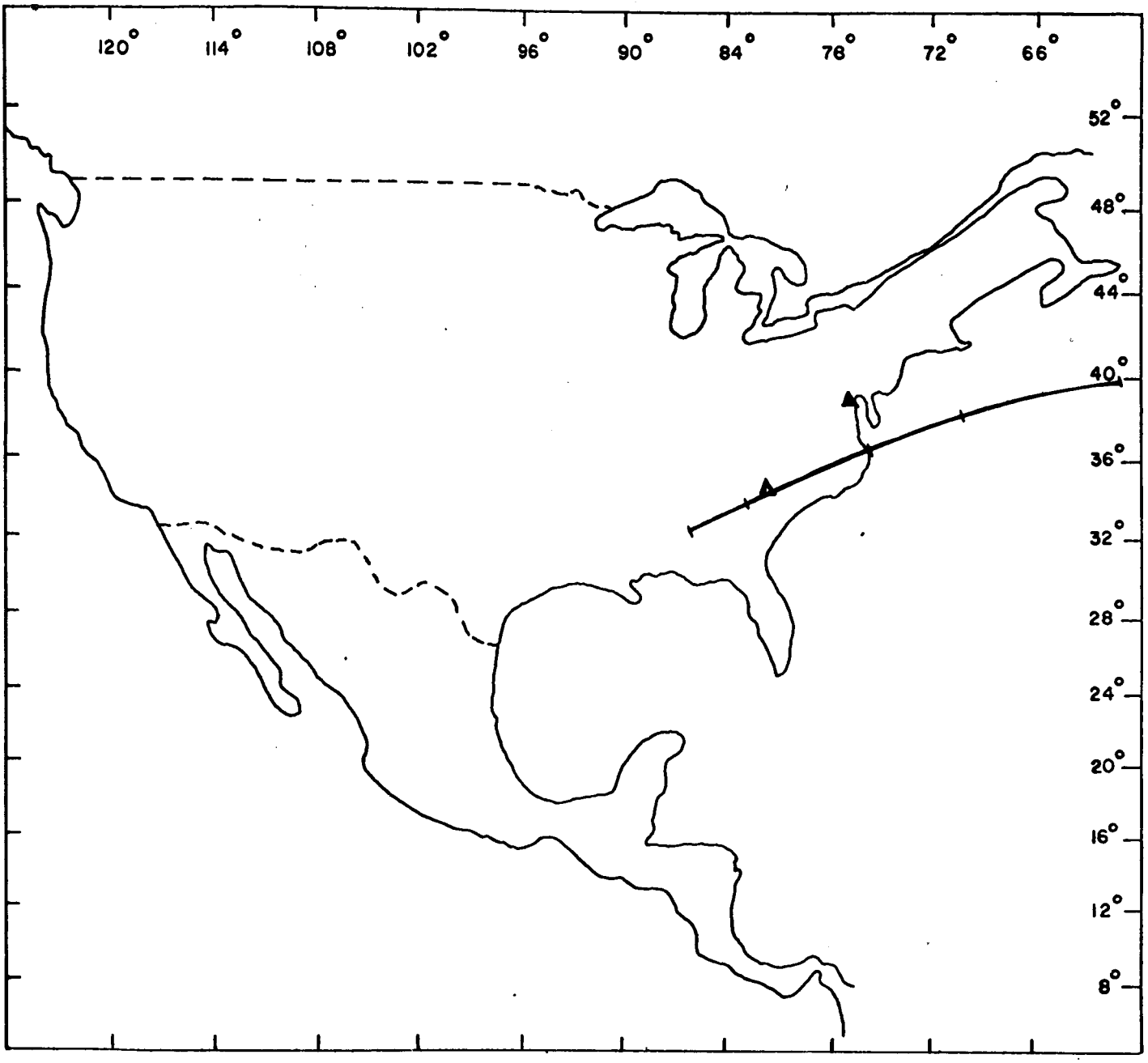

MAY 5, 1966

BASE TIME

0.0 HOURS
57.000 MINUTES
53.00200 SECONDS

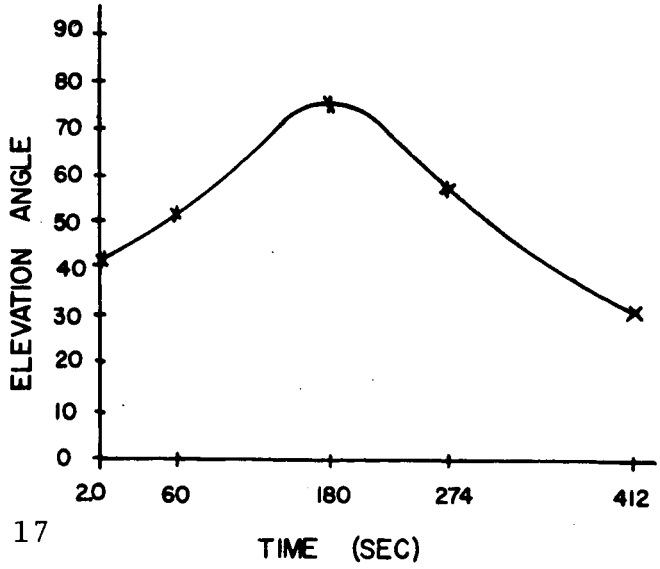

Figure 17

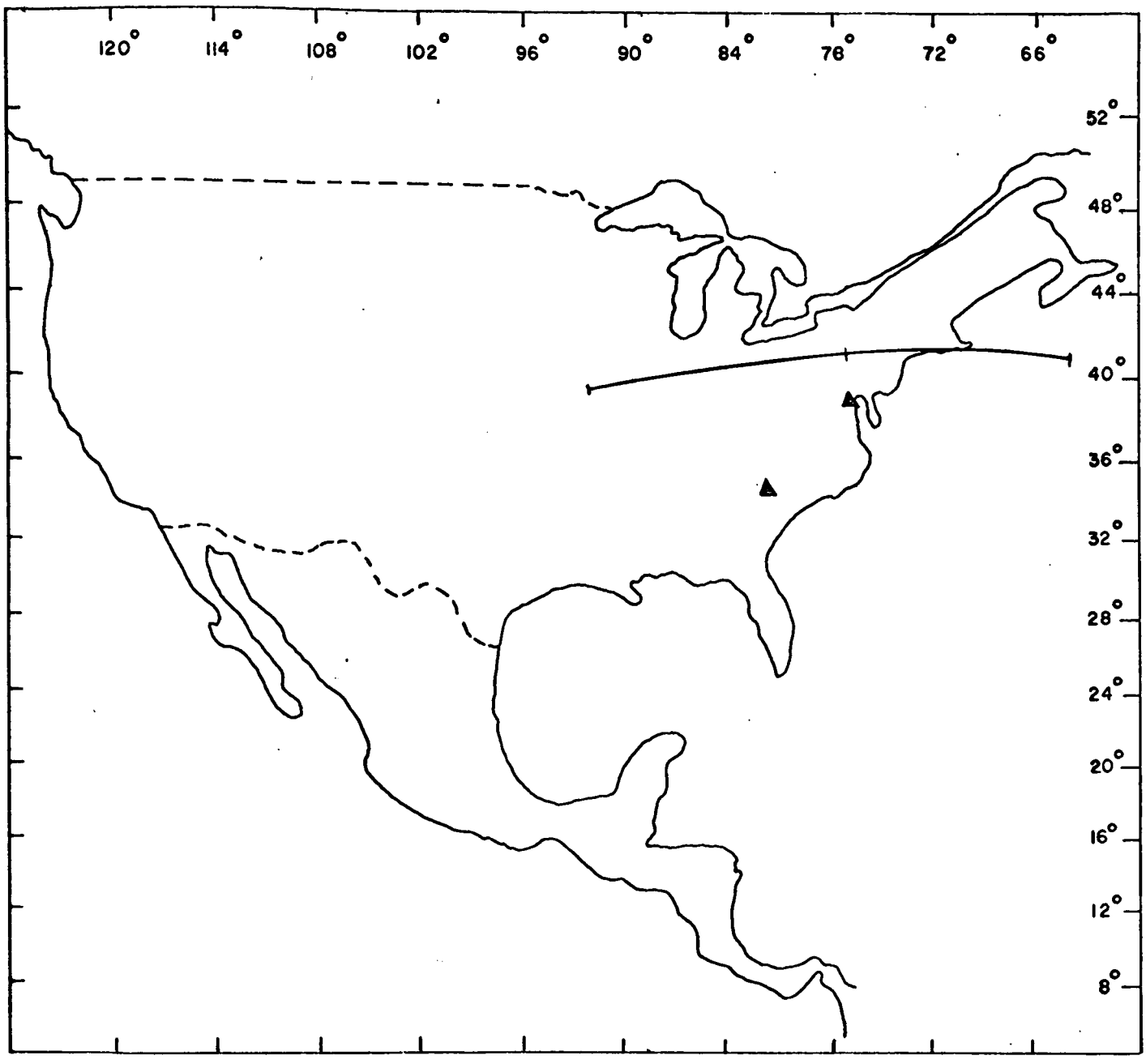

MAY 5, 1966

BASE TIME
2.000 HOURS
51.000 MINUTES
7.00000 SECONDS

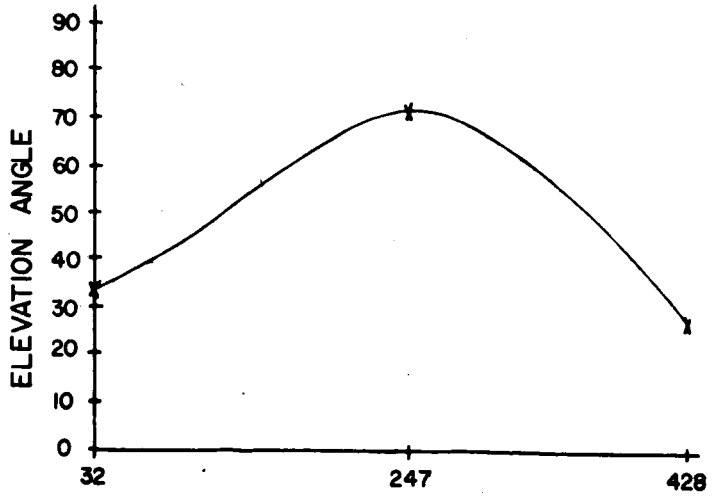

Figure 18

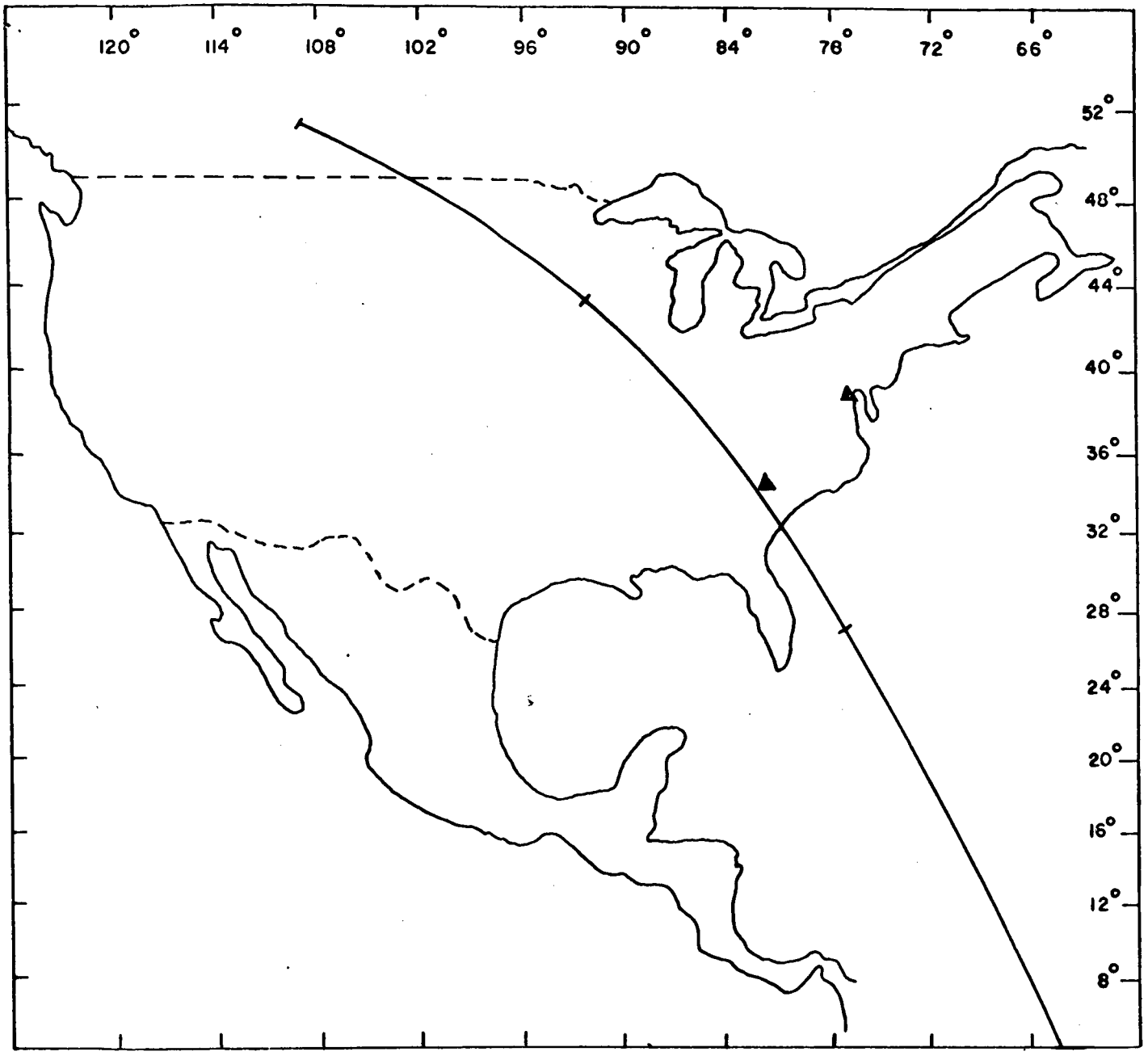
120°
114°
108°
102°
96°
90°
84°
78°
72°
66°
52°
48°
44°
40°
36°
32°
28°
24°
20°
16°
12°
8°

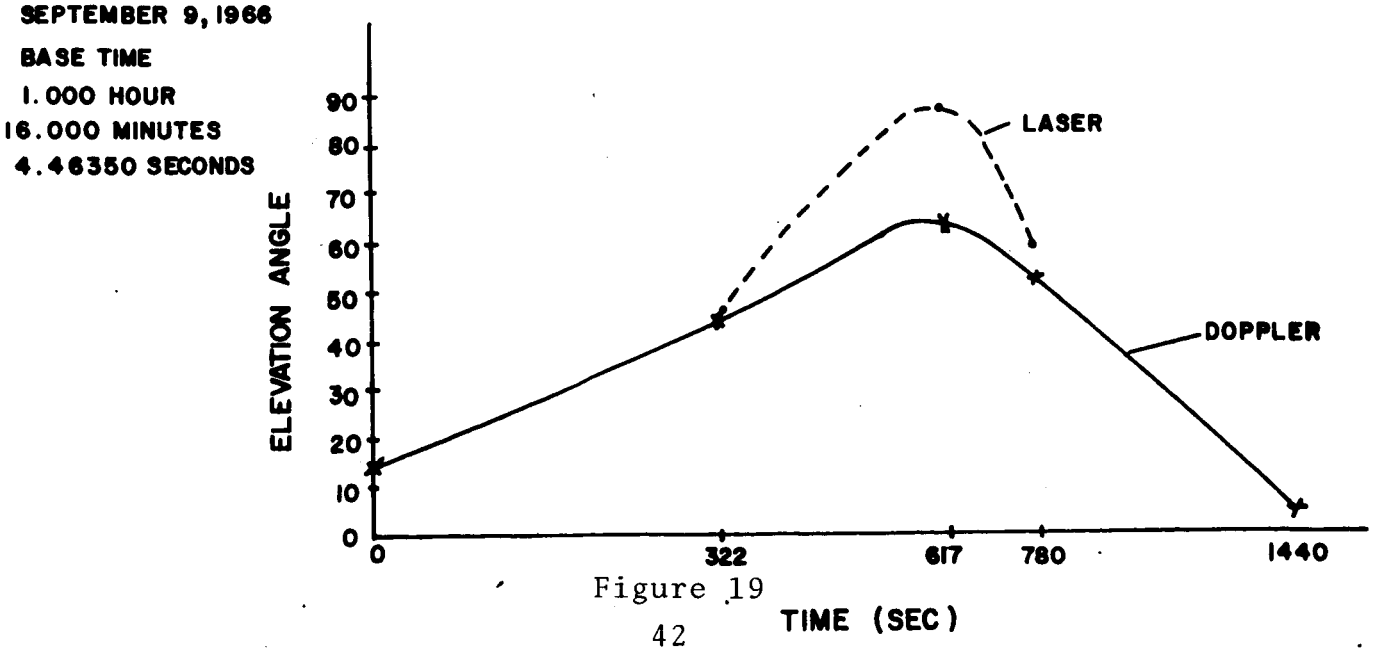
SEPTEMBER 9, 1966
BASE TIME
1.000 HOUR
16.000 MINUTES
4.46350 SECONDS
ELEVATION ANGLE
90
80
70
60
50
40
30
20
10
0
LASER
DOPPLER
0
322
617
780
1440
TIME (SEC)

Figure 19

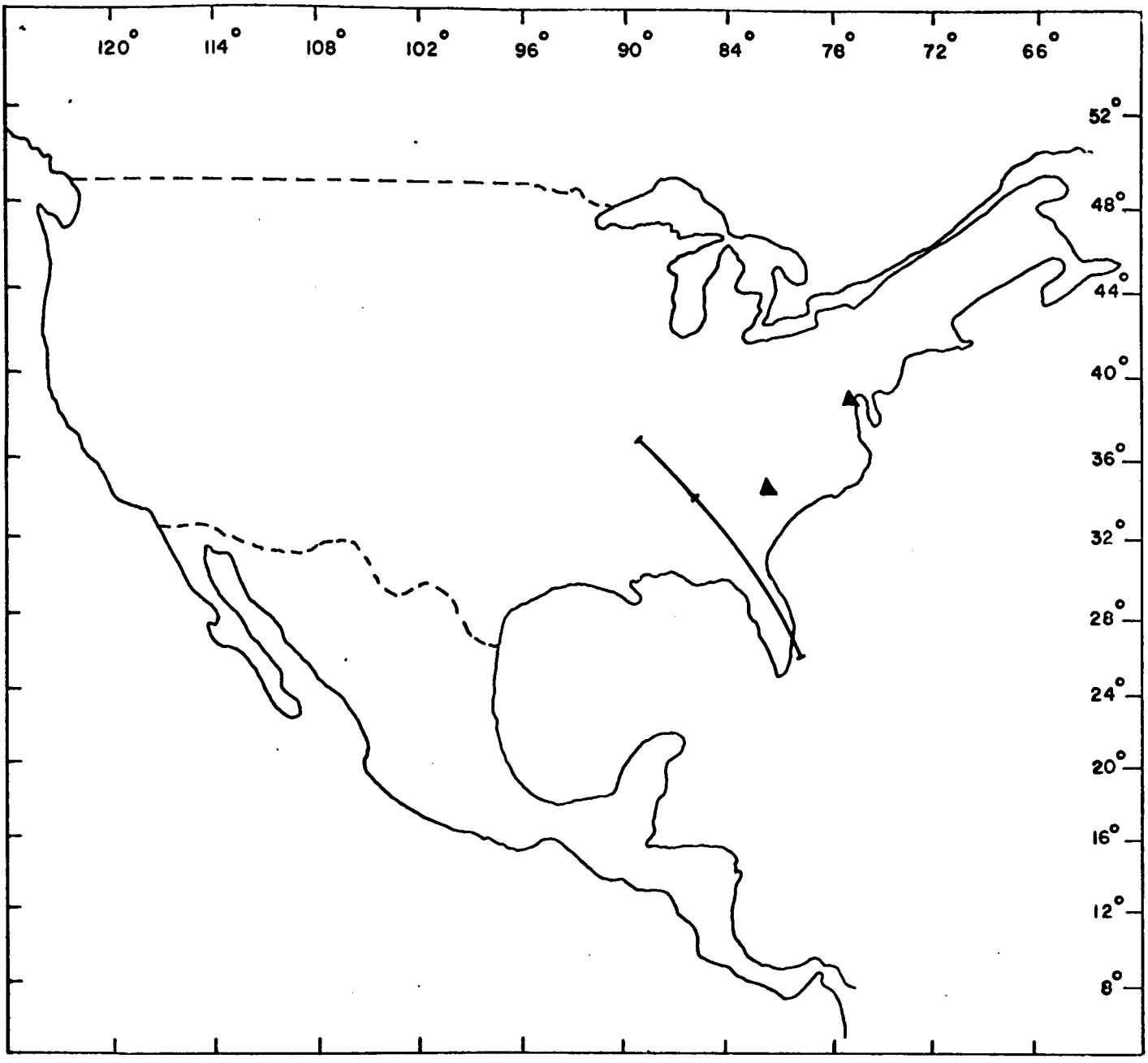

SEPTEMBER 10, 1966

BASE TIME

1.000 HOUR
27.000 MINUTES
50.00000 SECONDS

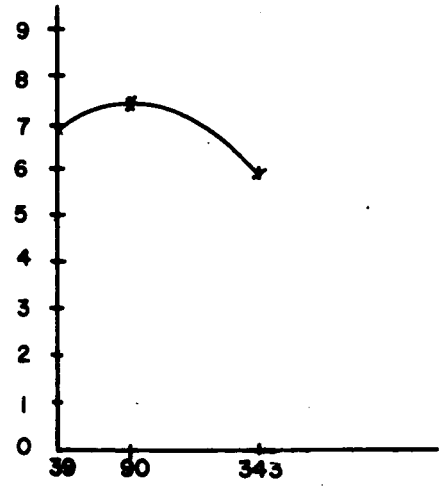

Figure 20

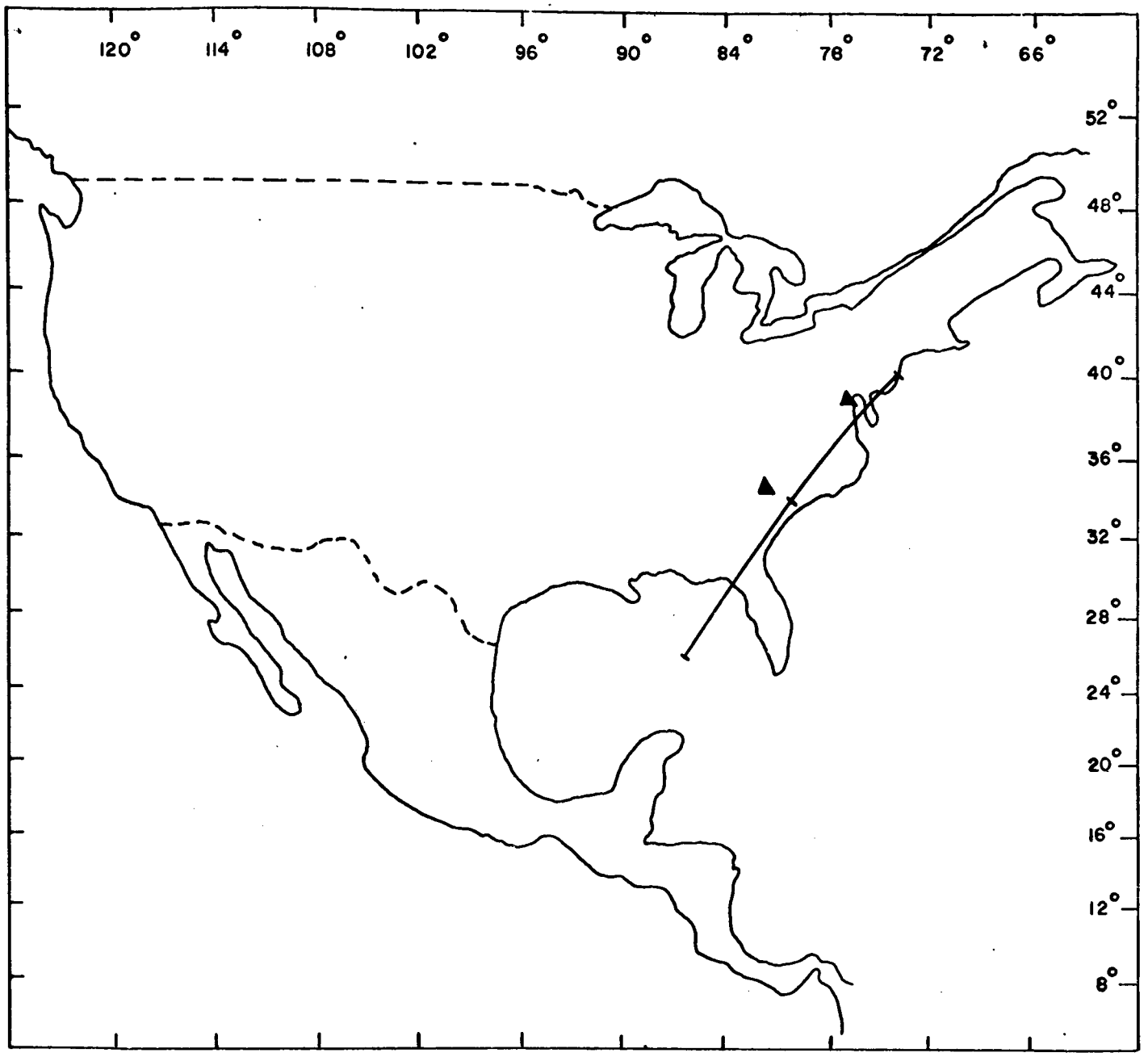

OCTOBER 6, 1966

BASE TIME
10.000 HOURS
27.000 MINUTES
52.00000 SECONDS

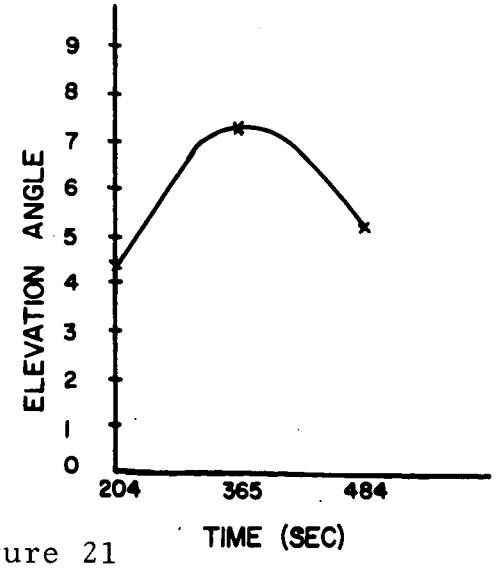

Figure 21

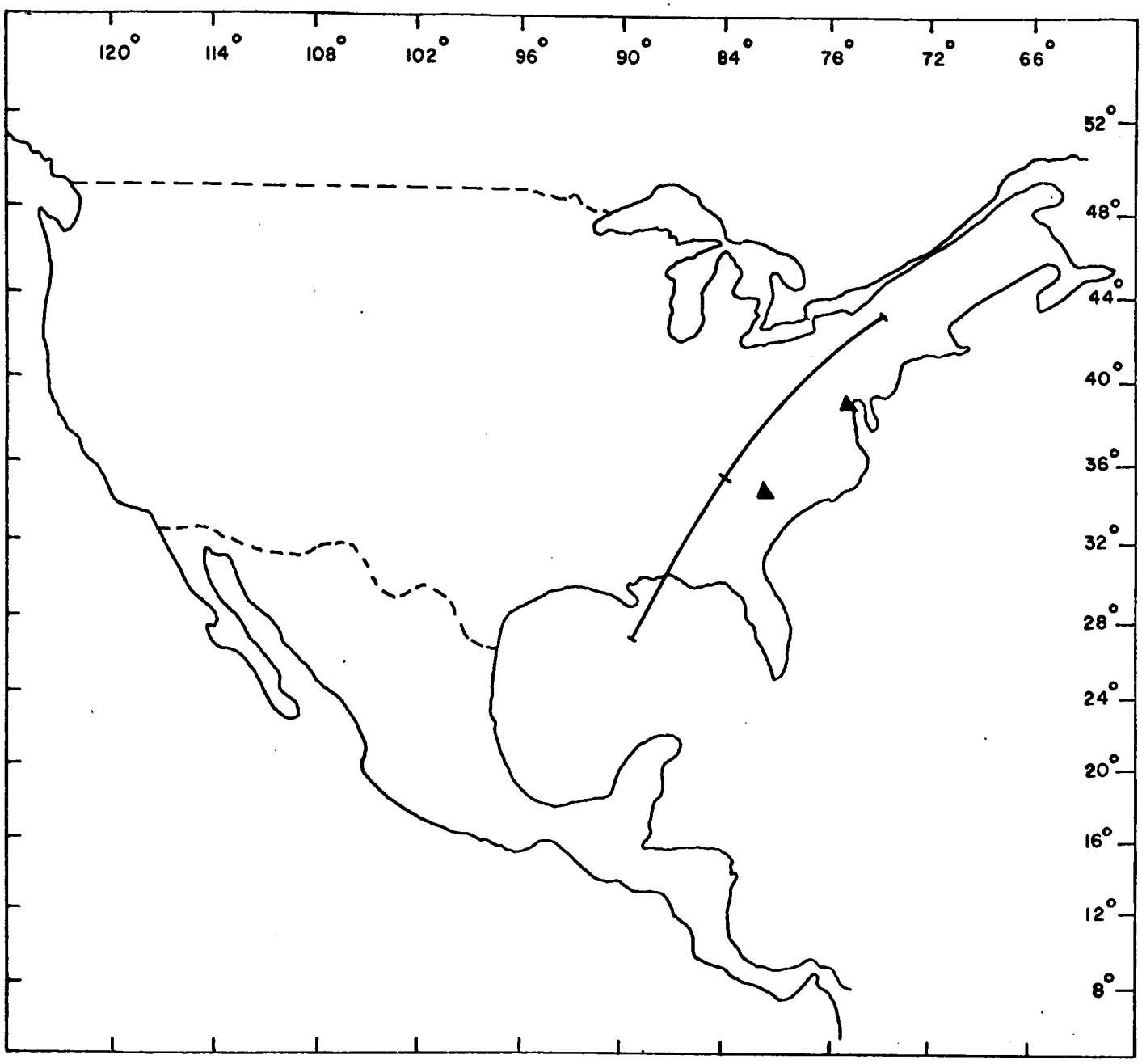

OCTOBER 7, 1966

BASE TIME

10.000 HOURS
35.000 MINUTES
25.00000 SECONDS

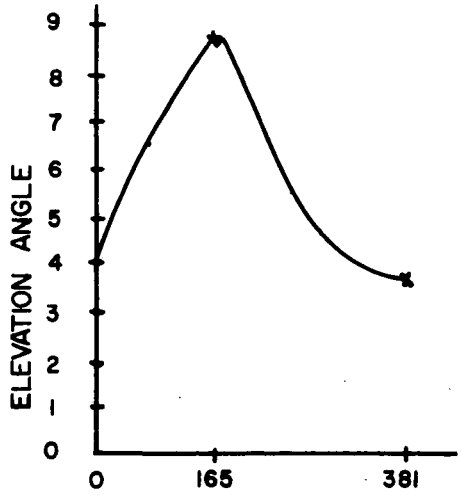

Figure 22

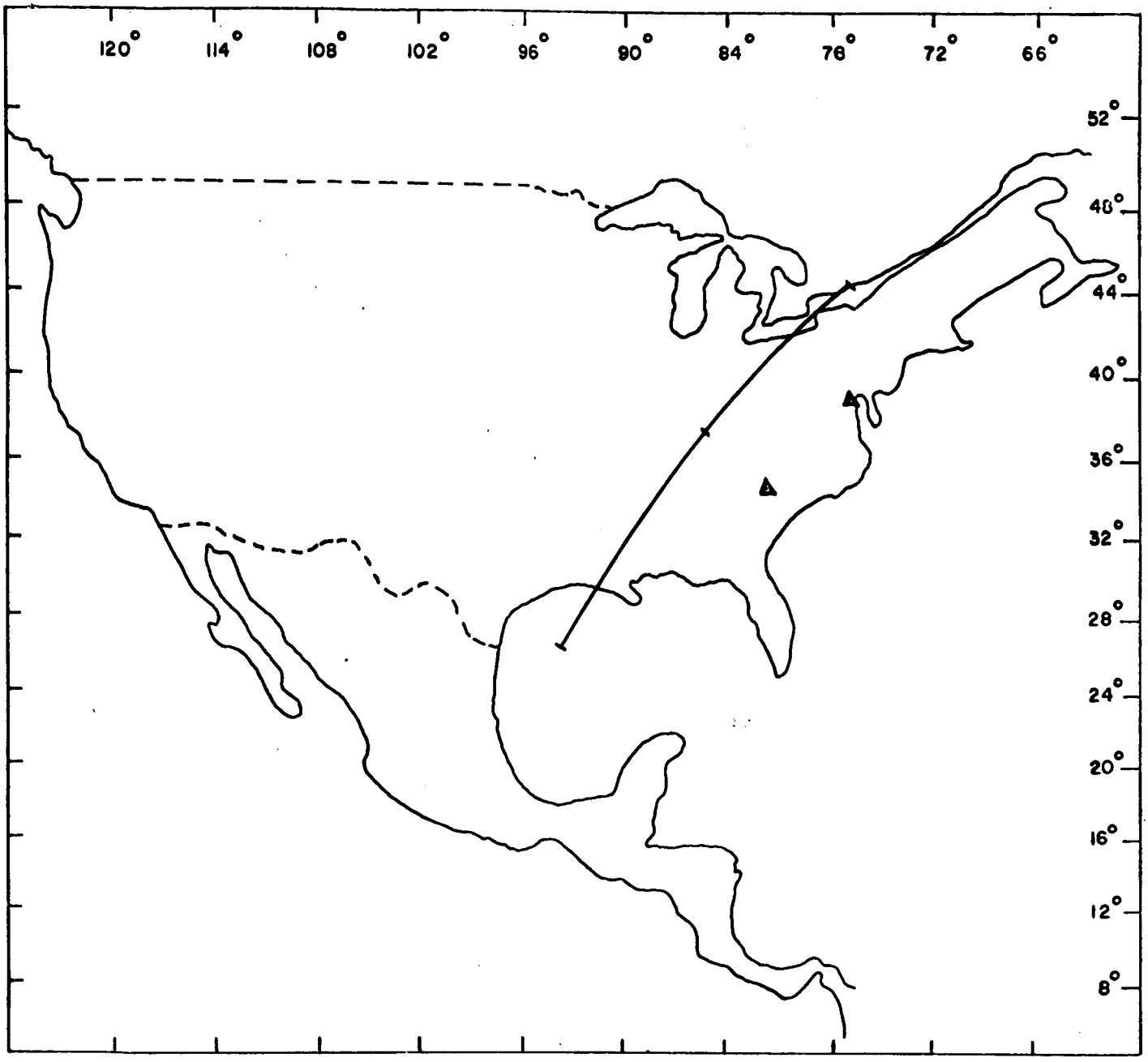

OCTOBER 8,1966

BASE TIME

10.000 HOURS
38.000 MINUTES
40.00000 SECONDS

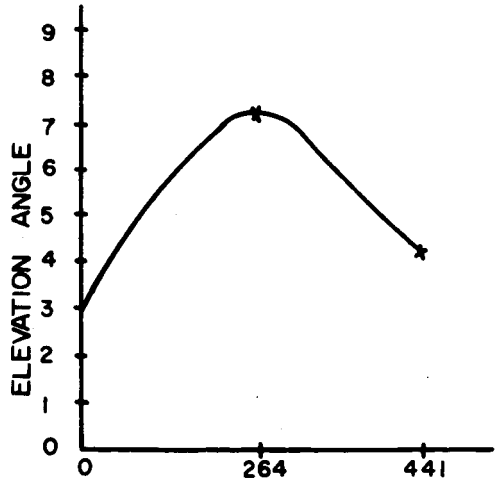

Figure 23

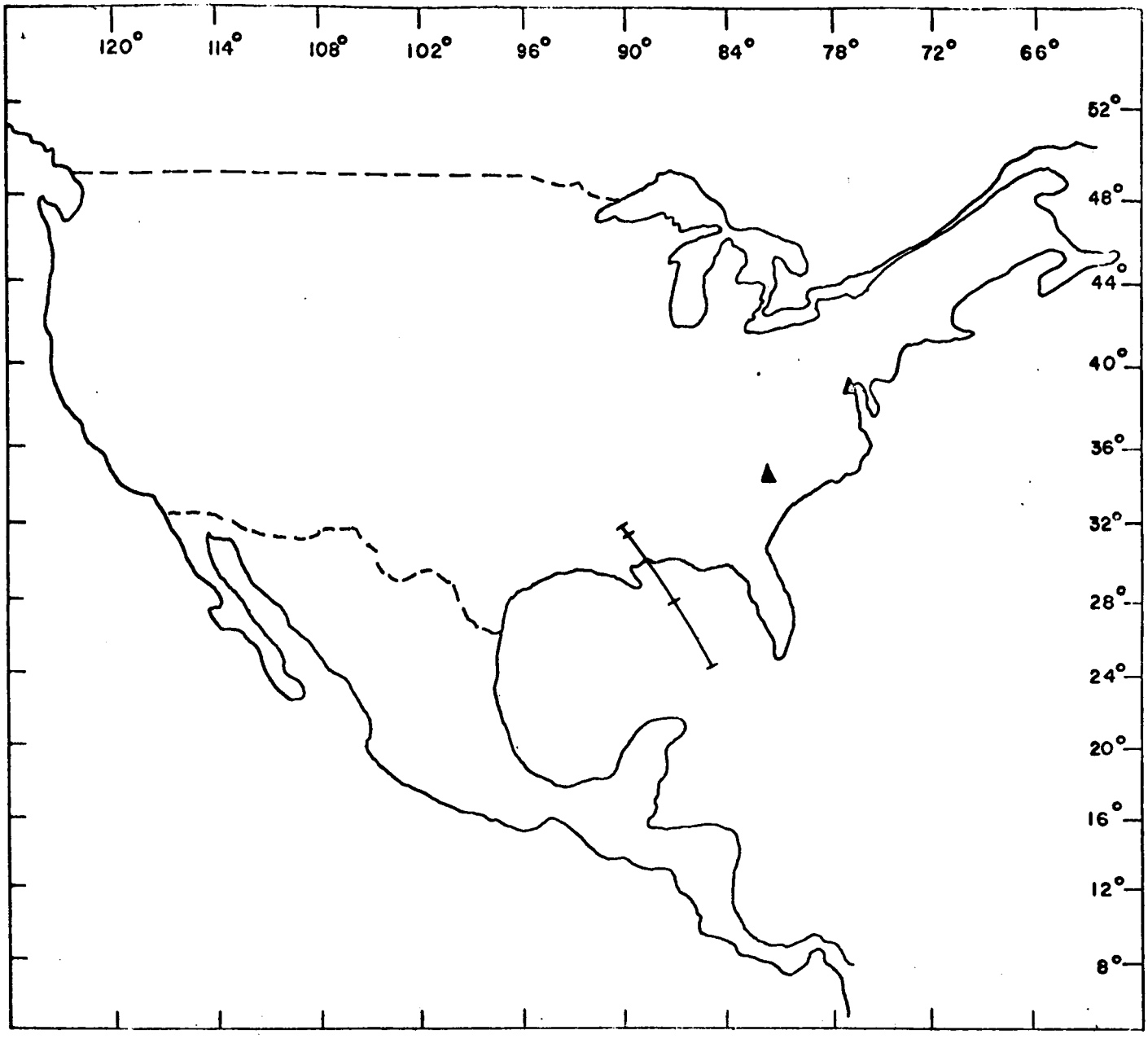

NOVEMBER 15, 1966

BASE TIME
11.000 HOURS
31.000 MINUTES
12.00000 SECONDS

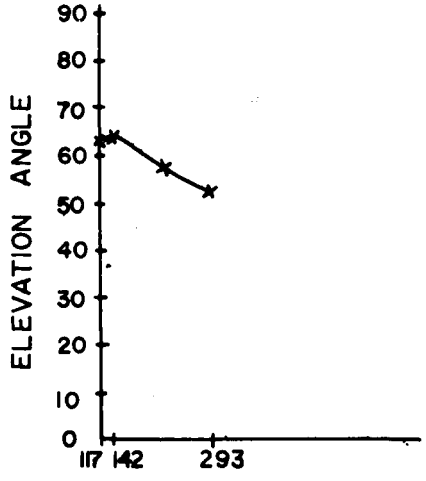

Figure 24

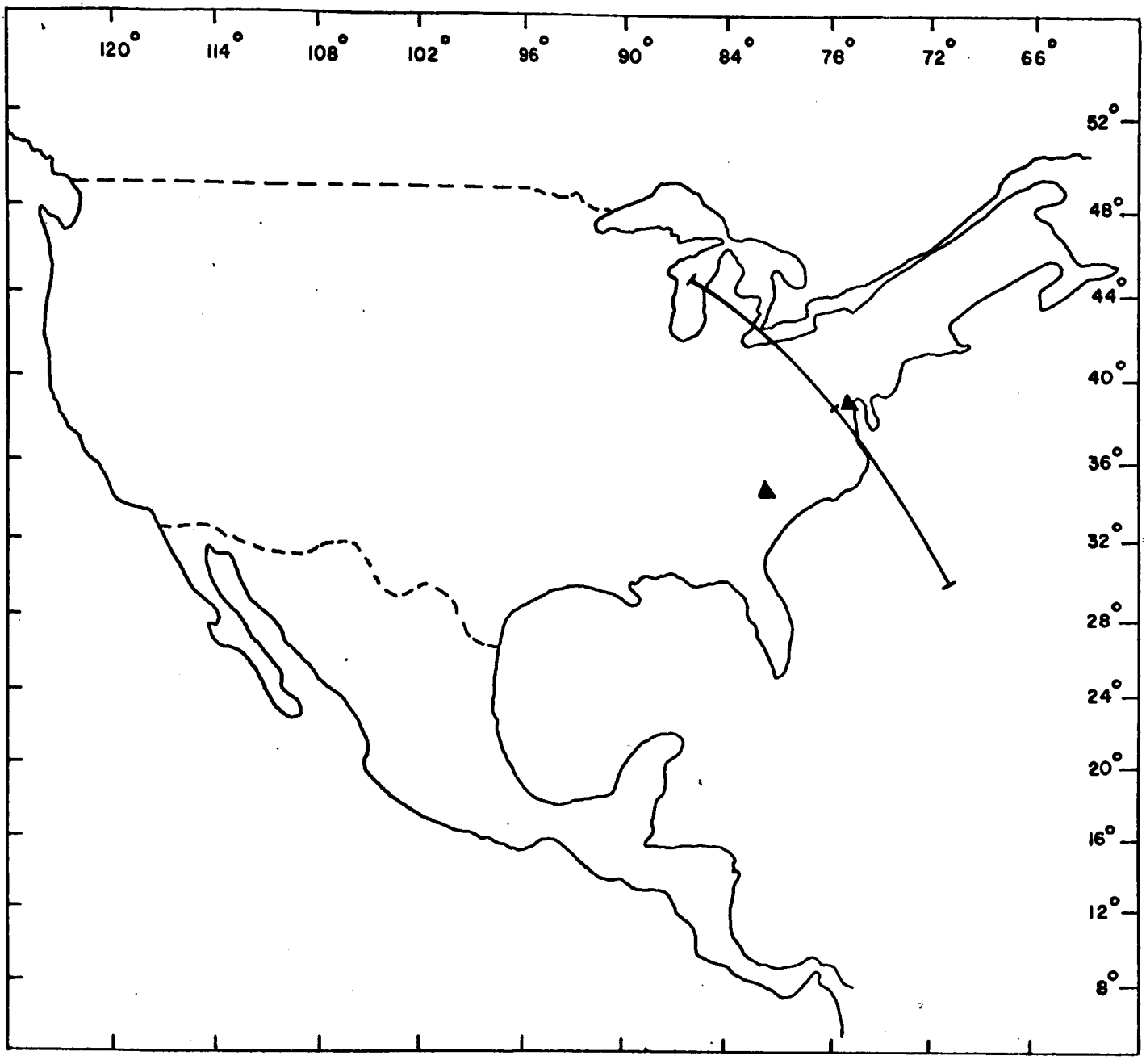

NOVEMBER 18, 1966

BASE TIME
9.000 HOURS
37.000 MINUTES
55.00000 SECONDS

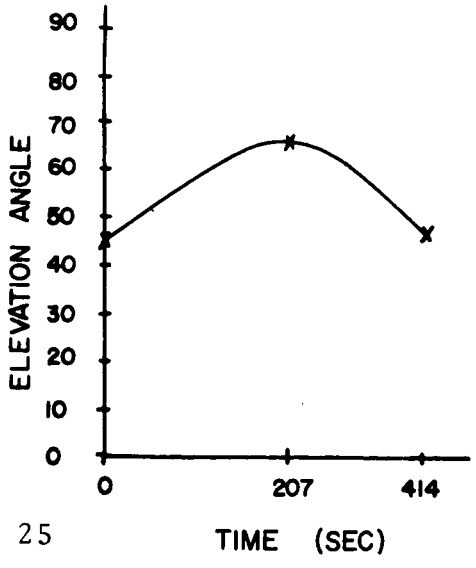

Figure 25

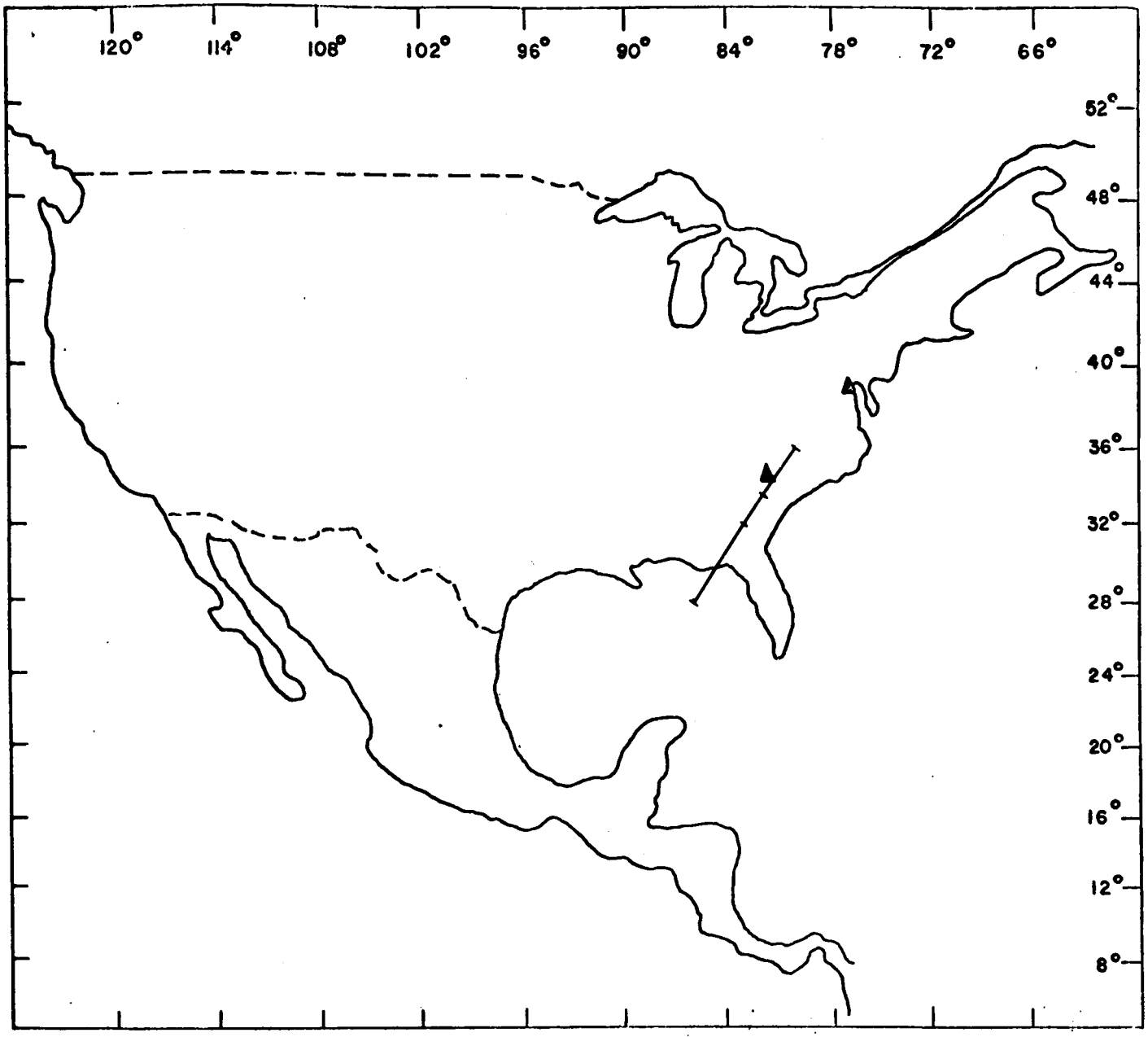

NOVEMBER 19,1966

BASE TIME

1.000 HOURS
12.000 MINUTES
8.00000 SECONDS

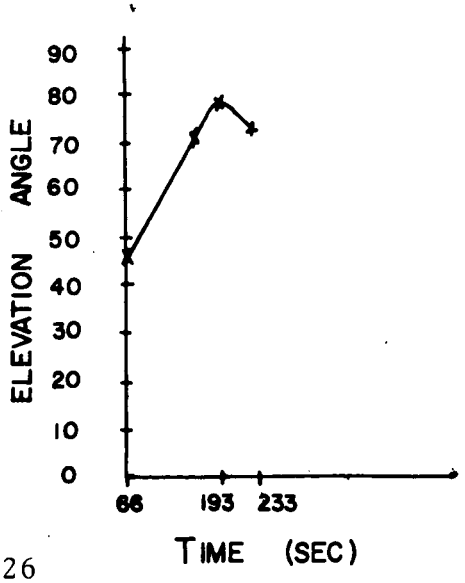

Figure 26

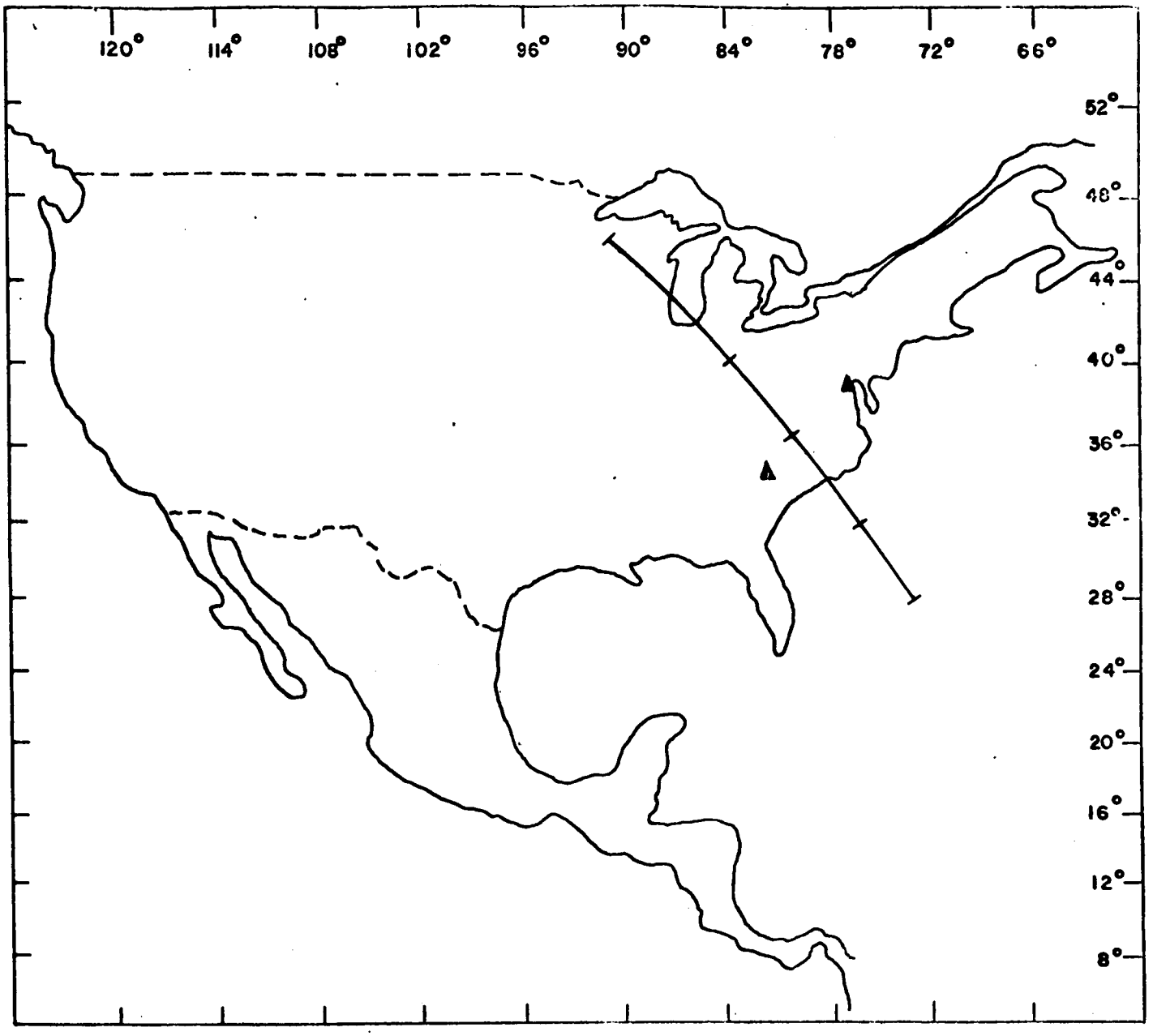

NOVEMBER 19, 1966

BASE TIME
9.000 HOURS
41.000 MINUTES
30.00000 SECONDS

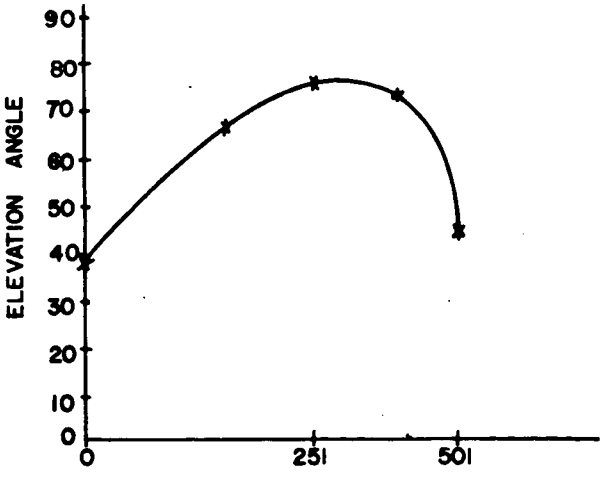

Figure 27

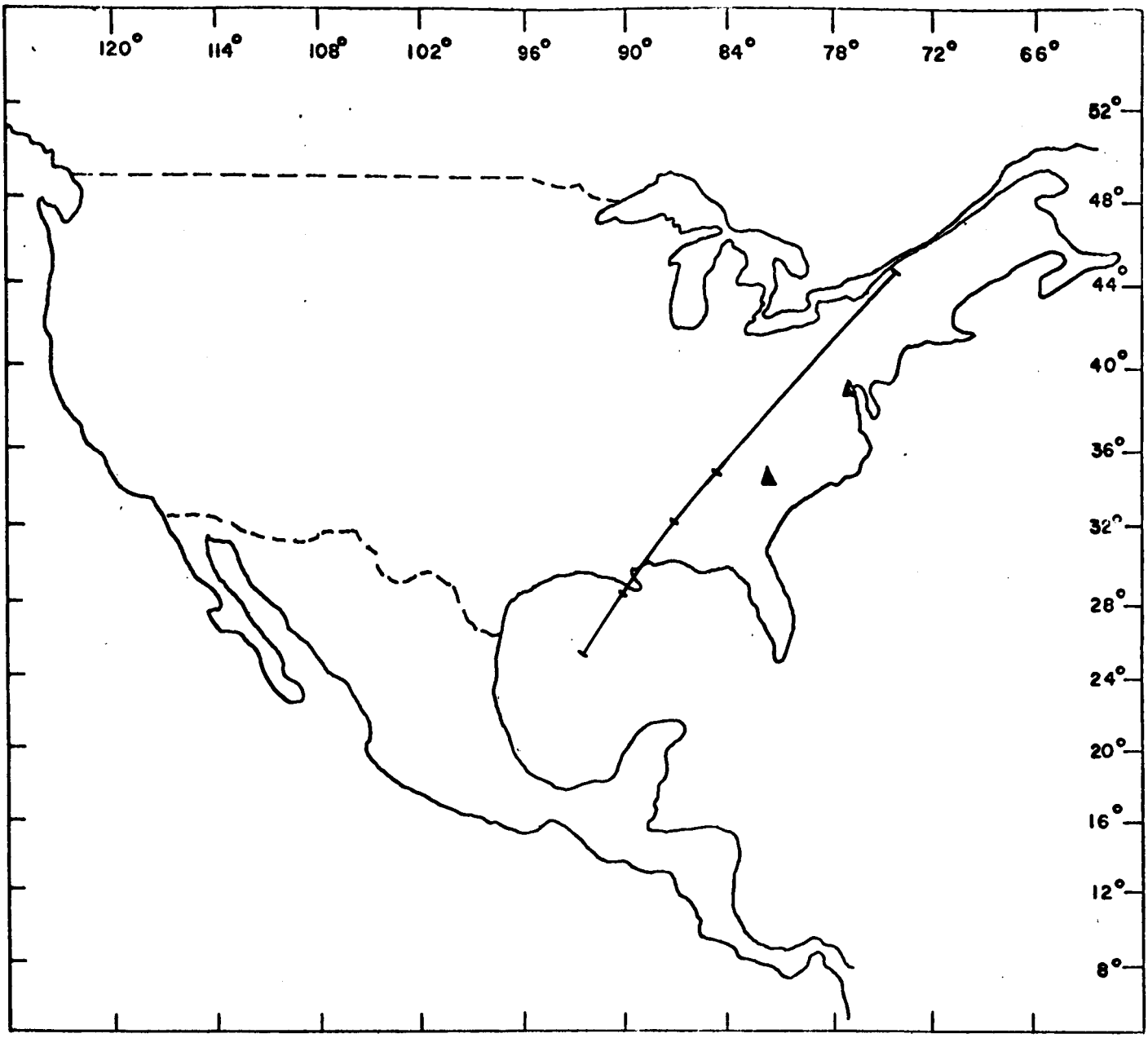

NOVEMBER 20,1966

BASE TIME

1.000 HOURS
16.000 MINUTES
1.00000 SECONDS

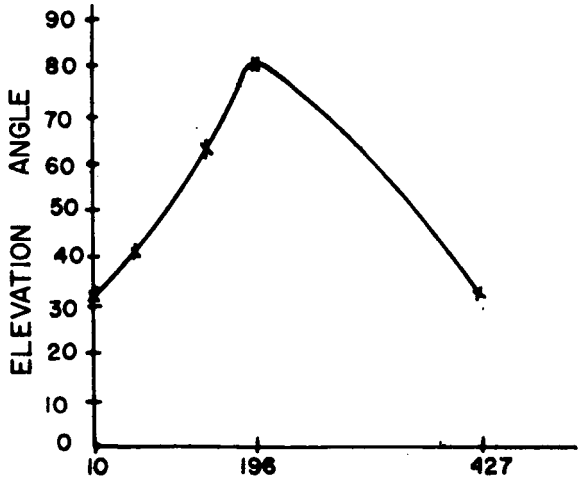

Figure 28

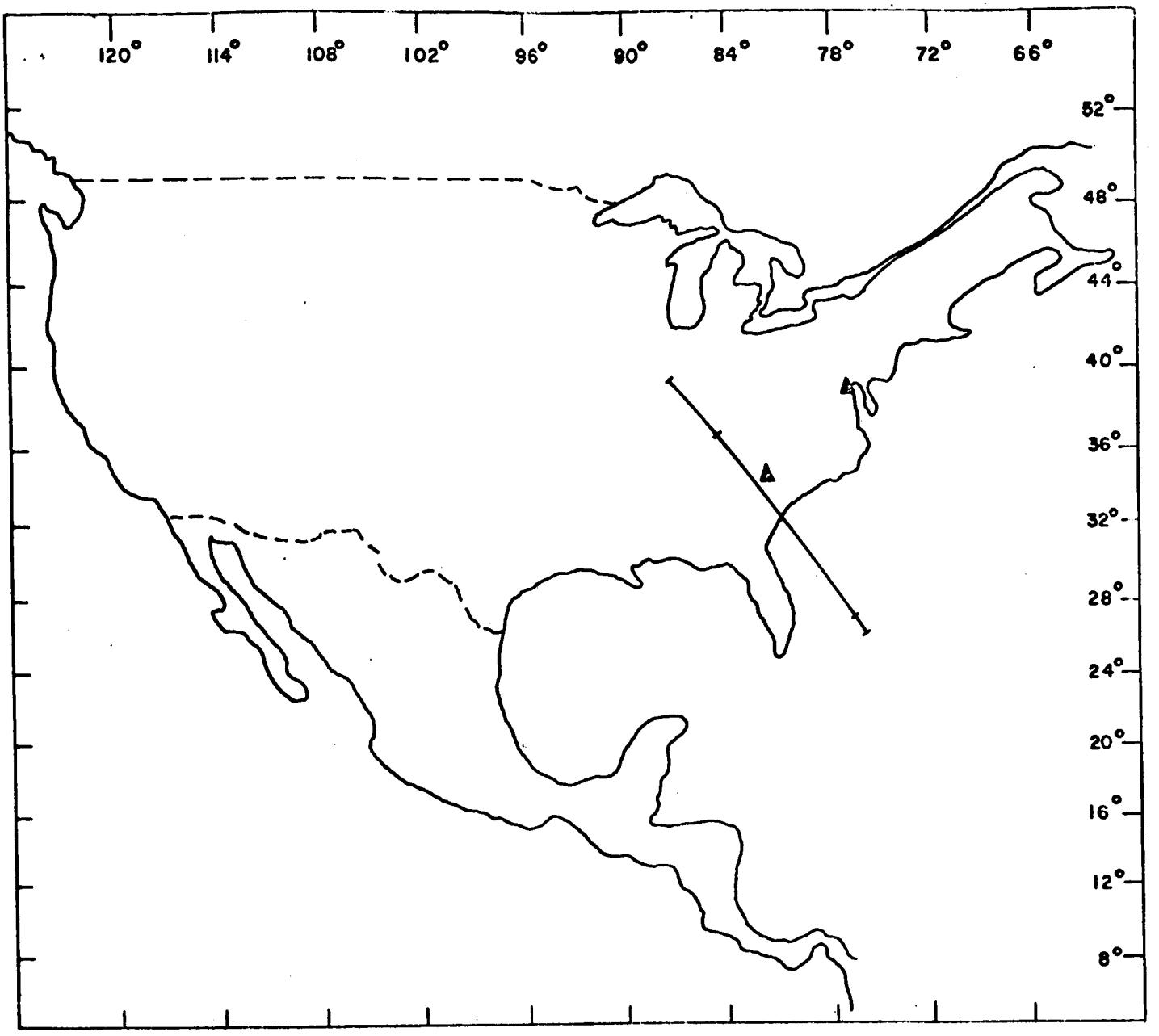

NOVEMBER 20,1966

BASE TIME
9.000 HOURS
48.000 MINUTES
28.00000 SECONDS

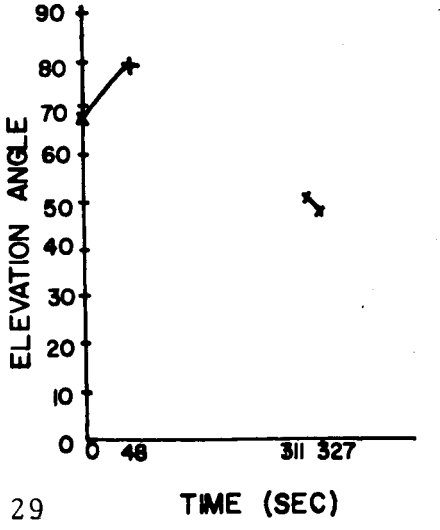

Figure 29

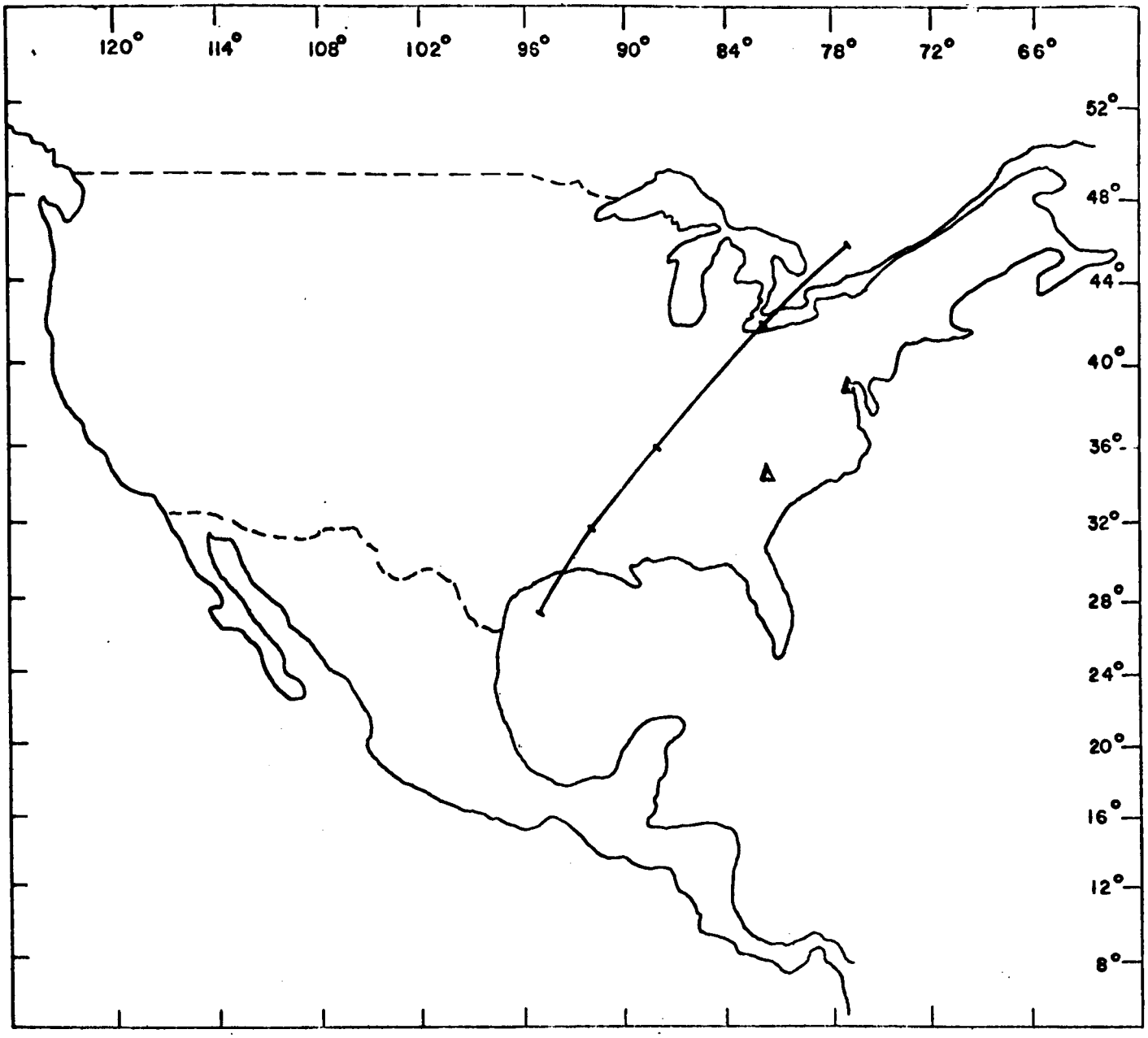

NOVEMBER 21,1966

BASE TIME
1.000 HOURS
20. 000 MINUTES
22.00000 SECONDS

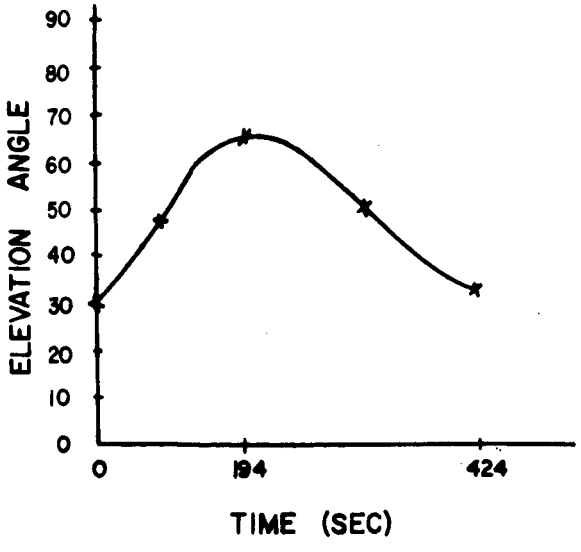

Figure 30

2. The root mean square of the range residuals are in most cases less than two meters. It is believed that this is a valid estimate of the noise content in the data for the present tracking system configuration.

3. The histograms of the residuals display a slight asymmetry toward the long range side. This asymmetry is associated with the variation in the return signal amplitude which triggers a threshold type detector. This variation in return signal strength appears as a variable delay in stopping the system clock causing the asymmetric distribution in the residuals in the positive direction.

3.2 Systematic Error Discussion

It is of interest to establish whether the results of Section 3.1 can be considered to be conclusive or if indeed the single station, range only solution is capable of masking one of a number of systematic errors or combinations of these biases.

In this study systematic errors of three types were considered.

1. The constant bias - a_1

2. The rate bias - $a_2 t$

3. The time bias - $a_3 \dot{R}$

Here t is the time elapsed from the epoch of elements, and $\dot{R}$ is the instantaneous range-rate of the satellite.

The systematic errors were applied to the range measurements such that the maximum value of any single bias was approximately 180 meters. The pass used in this study was the 8 October 1966 GEOS-A pass over Rosman, North Carolina, at $10^h\ 38^m$ GMT. The span of data covered 425 seconds and was made up of 305 data points. A maximum range-rate of 5 km/sec was assumed. With this information the bias coefficients a_1, a_2, and a_3 were chosen as:

$$a_1 = 180 \text{ meters}$$

$$a_2 = 0.412 \ \frac{\text{meters}}{\text{sec}} \qquad (3.5)$$

$$a_3 = 0.037 \text{ seconds}$$

The biases were applied to the data in the following manner:

Run No.	Bias	Comment
1	a_1	constant bias
2	$a_2 t$	rate bias
3	$a_3 R$	time bias
4	$a_1 + a_2 t$	constant + rate bias
5	$a_1 + a_3 \dot{R}$	constant + time bias
6	$a_2 t + a_3 \dot{R}$	rate + time bias
7	$a_1 + a_2 t + a_3 \dot{R}$	constant + rate + time bias

Each of the seven biased data sets was reduced exactly as the original data. Recall from Table 1 that this data after reduction had a root mean square range residual of 1.6 m meters about a mean residual of 0.01 meters. The residuals tested not significantly non-random with a normal deviate of 1.61.

The results of the analysis of the biased data runs are given in Table 2.

TABLE 2

Run No.	Mean of Residuals (m)	RMS of Residuals (m)	Normal Deviate
1	0.13	1.73	0.23
2	0.05	1.64	1.61
3	0.06	1.63	1.61
4	0.06	1.96	-0.80
5	0.14	1.73	0.0
6	0.17	1.64	1.38
7	0.15	1.96	-1.49

8 October 1966 Data Reduced With Simulated Systematic Errors

These results clearly indicate that any of the systematic errors introduced above in any combination can be effectively masked by a short arc single-station orbital fit. Whereas a short arc fit is a useful tool for evaluating the noise characteristics of an instrument, the orbital elements of this fit should not be taken as definitive. Moreover, short arc single-station fits are not powerful for systematic error investigations, particularly when only one principal measurement type is available.

3.3 Serial Correlation

The results of Section 3.2 show that individual as well as combinations of systematic errors of the most common types are completely masked in a single-station short arc fit. The apparent randomness leads one to ask whether serial correlation among the measurements might also be masked in a single-station solution. To test for this possibility, the following test was devised: The 8 October 1966 data, which previously checked out to be not significantly non-random with a noise level of 1.60 meters rms, was artificially correlated. A set of errors with mean zero and

standard deviation of fifty meters was generated in a Monte Carlo fashion. These independent errors, which we denote in time order by $(\varepsilon_1, \varepsilon_2, \varepsilon_3 \ldots \varepsilon_t)$ were correlated using the following expression:

$$\varepsilon_t^* = \alpha\varepsilon_{t-1} + \varepsilon_t \ , \qquad (3.6)$$

where α was chosen such that the correlation between ε_t^* and ε_{t-1}^* was 0.9. Having generated these correlated errors, the range measurements with the correlated errors added were subjected to a single station orbital fit. The resulting solution showed significantly non-random residuals (normal deviate - 6.5) with a noise level of 43 meters rms about a mean of 0.2 meter.

These results strengthen the previous conclusion that the laser provides independent measurements, even at the rate of one per second.

4.0 INTERCOMPARISON OF LASER AND DOPPLER DATA

Having established the internal consistency of the laser tracking data through the previous single-station solutions, we now establish the quality of the data by comparing it with data acquired from other geodetic tracking instrumentation. This is commonly done by reducing data from two or more systems tracking a given satellite where near-simultaneous data is available. A typical situation of this kind is depicted in Figure13, where the GSFC laser at Rosman, North Carolina, and the Applied Physics Laboratory Tranet Doppler station at Howard County, Maryland, were tracking GEOS-A. These data were obtained on 9 September 1966.

The major concern in reducing data from two or more systems in a common solution is to establish the proper weight for each type of measurement; i.e., each measurement must be assigned a weight which is inversely proportional to the square of standard error of the noise in the measurement. One means of estimating the noise is to reduce the data from each station individually, as was done in the case of the laser. This has the advantage of suppressing the effect of any systematic errors and of giving a valid estimate of the noise only.

4.1 Doppler Range-Rate Only Solution

Range-rate data available from the Tranet Doppler System was reduced in a single-station short arc solution similar to that used for the analysis of laser data.

The results of the reduction showed that the Doppler data acquired at the APL Howard County site had a noise level of .03 m/sec. Like the laser data, the Doppler data did not appear significantly non-random which indicated that bias errors, if any, were fitted out by adjustment of the orbit.

4.2 Laser-Doppler Combined Solutions

From the short arc solutions with laser only and Doppler only data, it is apparent, if not surprising, that the former solution, although capable of positioning the satellite with somewhat more accuracy than the range-rate solution, is considerably weaker in determining the satellite velocity than the Doppler data. The combined solution with properly weighted data may well provide the state-of-the-art in orbit determination. As an initial step, a combined solution was

obtained using as relative weights the results of the laser only and Doppler only solutions.

The results are summarized below.

	RMS Range	RMS Range-Rate	Normal Dev Range	Normal Dev Range-Rate
Laser only solution	1.6 m		-2.0	
Doppler only solution		.03 m/sec		-1.89
Laser/Doppler solution	1.6 m	.04 m/sec	-1.79	-4.11

The table shows that the Doppler RMS increases slightly, and the residuals exhibit a systematic trend. Additional studies are being made to identify the source of this systematic trend.

APPENDIX A

PRE-PROCESSING PROCEDURE

The data available from the GSFC Laser Tracking System are the following:

1. Satellite number
2. Year, month, day of observation
3. Hour, minute of observation
4. Second (on the even WWV received second) of initiation of laser energizing pulse
5. Delay from even second (4) to initiation of laser radiation
6. Round trip time of laser pulse from station to satellite
7. Azimuth (except BE-C)
8. Elevation (except BE-C)
9. Total delay in signal due to telescope optical path length and delay through photomultiplier tube.

Item (9) is measured against over a precisely calibrated range before and after each pass.

We denote the nominal observation time represented by items (2), (3), and (4) as T, while items (5) and (6) are respectively denoted by Δt and t_R. The delay (9) is denoted by t_D.

A.1 Computation of Time of Observation

The time of the observation is somewhat ill-defined in that the question to be answered is, "at what time was the range to the satellite that which was measured?" Because the satellite is in continuous motion, this is not exactly determinable. To a good approximation, this time is one-half the round trip interval, t_R, added to the time at which the laser began to radiate. However, the measured round trip interval is too long by an amount t_D; therefore, the time of observation is given by:

$$T_o = T + \Delta t + \frac{1}{2} (t_R - t_D) \qquad (A.1)$$

A.2 Conversion of Time Interval to Range

The range is computed from the round-trip time interval adjusted for the delay t_D by multiplying by the speed of light, c, divided by two. The value used for the speed of light is

$$C = 2.997925 \times 10^8 \text{ meters/second;} \quad \text{(A.2)}$$

thus

$$R = \frac{c}{2} (t_R - t_D) . \quad \text{(A.3)}$$

A.3 First Order Refraction Correction to Range

The conversion of time interval to range given in A.2 uses the speed of light in vacuum; however, the light pulse considered here traverses varying distances through the atmosphere depending on the elevation angle of the satellite from the observing station. The intervening atmosphere, which increases the optical path from the station to the satellite, causes the measured range, R, to be longer than the true slant range, R_c.

Figure 31 shows that to a first approximation the distance traversed through the atmosphere increases as cse E_o, where E_o is the elevation angle*. If it is further assumed that the atmospheric density decreases exponentially with altitude, the index of refraction takes the form

$$N_s = N_o \exp\left(-\frac{h}{H}\right) \qquad (A.4)$$

where

h = altitude

H = scale height ≃ 7.5 kilometers

$N_o = (n_o - 1)$

$N_s = (n_s - 1)$

and

n_o = ground level index of refraction

n_s = index of refraction at the satellite.

---

* This approximation is good for $E_o > 10°$.

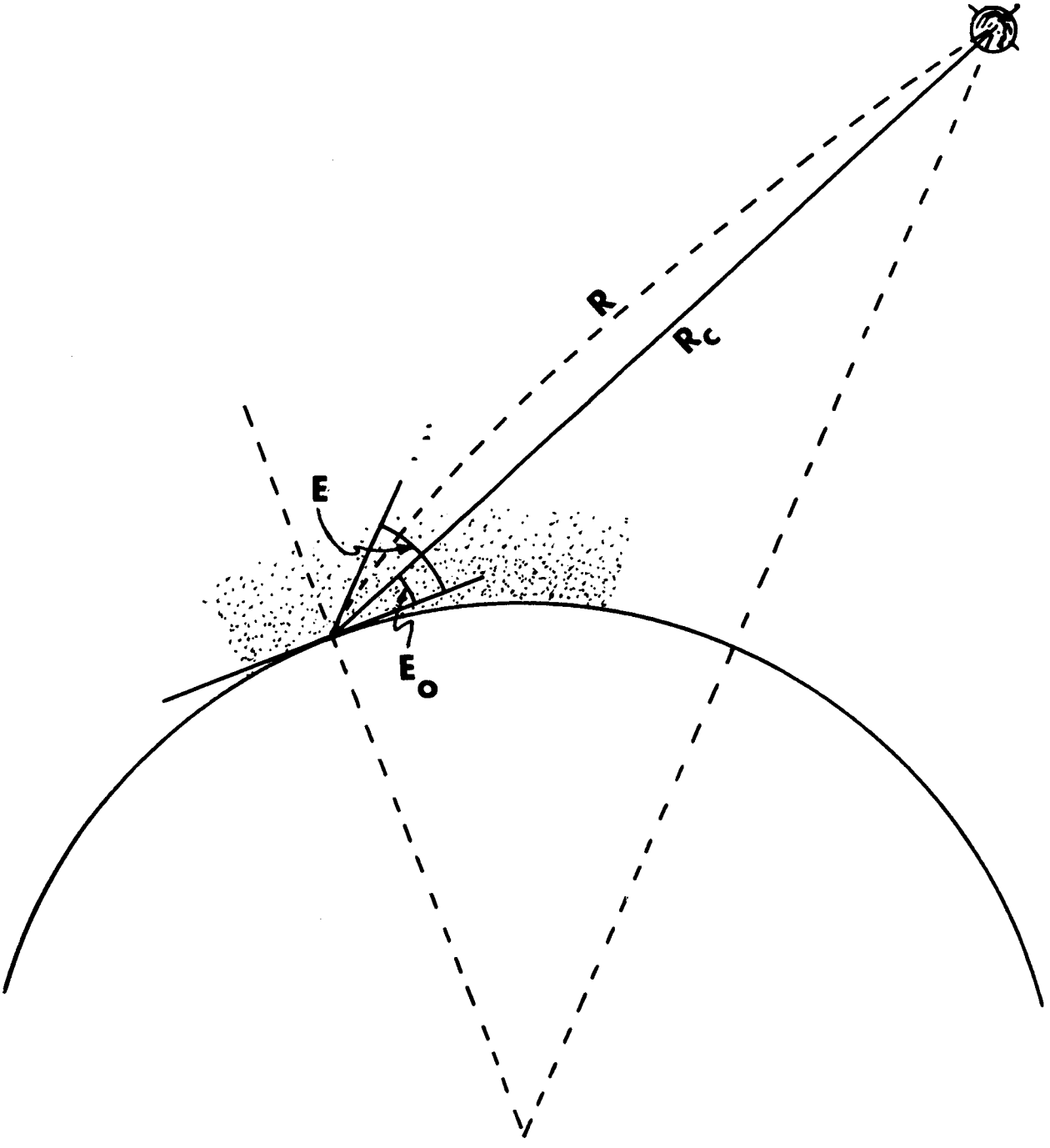
R
R_c
E
E_o

To compute the difference between the optical path length and true range we will first consider the situation where the satellite is directly above the station at an altitude h. The optical path length is

$$R = \int_o^h n_s \, dh = \int_o^h \left[1 + (n_o - 1) e^{\frac{-h}{\bar{H}}}\right] dh \quad (A.5)$$

$$R = h + (n_o - 1) \, H \, (1 - e^{\frac{-h}{\bar{H}}}); \quad (A.6)$$

whereas,

$$R_c = h. \quad (A.7)$$

Therefore, the first order correction to the measured range is

$$\Delta R = R - R_c = (n_o - 1) \, H \, (1 - e^{\frac{-h}{\bar{H}}}) \, . \quad (A.8)$$

For the case of interest h >> H thus

$$\Delta R = (n_o - 1) \quad H \ . \tag{A.9}$$

A nominal ground level index of refraction for the red end of the spectrum is 1.0002916; consequently, using a scale height of 7.5 km., we find

$$\Delta R = 2.1 \text{ meters} \ . \tag{A.10}$$

If we now take into account the increase in atmosphere traversed with decreasing elevation angle, we find

$$\Delta R = 2.1 \csc E_o \text{ meters} \ . \tag{A.11}$$

In the case of analyzing BE-C data, 4 and 5 May 1966, where no elevation angle information was available, a preliminary short arc was fit to the range data, and the elevation angles were computed for use in the refraction correction.